

This is the **accepted version** of the article:

Villa, Andrea; Daza, Juan D.; Bauer, Aaron M; [et al.]. «Comparative cranial osteology of European gekkotans (Reptilia, Squamata)». *Zoological Journal of the Linnean Society*, Vol. 184, issue 3 (Nov. 2018), p. 857–895. DOI 10.1093/zoolinnean/zlx104

This version is available at <https://ddd.uab.cat/record/237520>

under the terms of the  ^{IN} COPYRIGHT license

Comparative cranial osteology of European gekkotans (Reptilia, Squamata)

Andrea Villa^{1,*}, Juan D. Daza², Aaron M. Bauer³, Massimo Delfino^{1,4}

¹ Dipartimento di Scienze della Terra, Università di Torino, Via Valperga Caluso 35, 10125 Torino, Italy.

² Department of Biological Sciences, Sam Houston State University, 1900 Avenue I, Huntsville, Texas 77341, USA.

³ Department of Biology, Villanova University, 800 Lancaster Avenue, Villanova, Pennsylvania 19085, USA.

⁴ Institut Català de Paleontologia Miquel Crusafont, Universitat Autònoma de Barcelona, Edifici ICTA-ICP, Carrer de les Columnes s/n, Campus de la UAB, 08193 Cerdanyola del Vallès, Barcelona, Spain.

Cranial osteology of European gekkotans

*Correspondence to: Andrea Villa, Dipartimento di Scienze della Terra, Università di Torino, Via Valperga Caluso 35, 10125 Torino, Italy. +390116705193

E-mail address: a.villa@unito.it

ACKNOWLEDGEMENTS

Authors are grateful to Simona Cavagna (University of Torino) for help in SEM analysis and imaging, and to two reviewers for improving an earlier version of the manuscript with their comments. This research received support from the SYNTHESYS Project <http://www.synthesys.info/> which is financed by European Community Research Infrastructure Action under the FP7 "Capacities" Program. Access to the collections of NHMW was possible thanks to a Synthesys grant (AT-TAF-4591) to AV. MD supported by Fondi di Ateneo dell'Università di Torino (2014-2015), Generalitat de Catalunya (2014 SGR 416 GRC and CERCA Program), and Spanish Ministerio de Economía y Competitividad (CGL2016-76431-P). AMB was supported by National Science Foundation grant DEB 1555968. JDD was supported by National Science Foundation grant DEB 1657648 and Sam Houston State University.

ABSTRACT

Comparative osteology of European lizards, and of European geckos in particular, is poorly known, resulting in problems when trying to determine to species isolated bones found as fossils or as remains of prey in scats or pellets. In order to partly solve this issue, we here present a detailed comparative analysis of the cranial bones of the four most broadly distributed species of European gekkotans: *Euleptes europaea*, *Hemidactylus turcicus*, *Mediodactylus kotschyi* and *Tarentola mauritanica*. The skulls of these species display both a set of features that are typical for geckos in general and unique features that can be employed to identify isolated bones of all considered species. Diagnostic differences are found in almost every bone (except the squamosal, epipterygoid and stapes), leading to the creation of a detailed diagnostic key. The dentition also displays some interspecific differences, even though all four species share a similar general tooth morphology, with pleurodont teeth provided with two parallel cutting edges separated by a groove-like space. Such a dentition is consistent with an arthropod-based diet.

Keywords: Comparative anatomy - *Euleptes europaea* - *Hemidactylus turcicus* - *Mediodactylus kotschyi* - *Tarentola mauritanica*

INTRODUCTION

Gekkota is a widely distributed group of squamates, collectively called geckos and including more than 1660 living species in seven families (Uetz & Hošek, 2016). They occupy a wide range of habitats, ranging from forested areas to deserts, and some species may be conspicuously anthropophilic (Davis, 1974; Howard & Parmerlee, 2001; Newbery & Jones, 2007; Bauer, 2013). Although many geckos are terrestrial, the group is perhaps best known for the ability of a plurality of species to climb using adhesive toepads that function through both friction and van der Waals forces (Russell, 2002; Autumn et al., 2002; Gamble et al., 2012). The majority of geckos are insectivorous, although some species also include nectar, fruit and vertebrates, including other lizards, in their diet (Daza et al., 2009; Vitt & Caldwell, 2009). Geckos are primarily nocturnal, although there are several hundred secondarily diurnal species and transitions between activity periods has occurred throughout the history of the clade (Röll, 2001; Gamble et al., 2015).

Our current knowledge of the comparative osteology of European lizards is, in general, rather scattered (Villa et al., 2017). Previous dedicated studies have covered a few species of lacertids and anguids (e.g., Klemmer, 1957; Arnold 1989; Barahona & Barbadillo, 1997, 1998; Arnold, Arribas & Carranza, 2007; Klembara, Hain & Dobiašová, 2014; Klembara et al., 2017) or specific taxa useful for the identification of fossil remains (e.g., Blain, 2009; Čerňanský, Klembara & Smith, 2016; Klembara & Rummel, 2016; Čerňanský & Smith, 2017). For a wider survey of literature dealing with this topic, see Villa et al. (2017). Osteological studies on European geckos include general descriptions of *Tarentola mauritanica* (Ficalbi, 1882; Wellborn, 1933; Rieppel, 1984), chondrocranial descriptions of *Tarentola mauritanica* and *Hemidactylus turcicus* (Kamal, 1961, 1965), analysis of cranial joints of *Hemidactylus turcicus*, *Mediodactylus kotschy*, and *Tarentola mauritanica* (Mezzasalma, Maio & Guarino, 2014), and recently a detailed study of the development of osteoderms in *Tarentola mauritanica* (Vickaryous, Meldrum & Russell, 2015).

Although some of these works provide some level of detail in their descriptions of cranial elements, none offer element-by-element descriptions and illustrations that would facilitate the differential

determination to species of isolated bones found in a palaeontological or zooarchaeological context or in or scats or pellets.

Geckos have been found in palaeontological assemblages (Daza, Bauer & Snively, 2014) and have been recovered from owl pellets, representing the most common prey item among reptiles (Roulin & Dubey, 2012). The identification of their bones or fossils has typically been based on few characters and has usually been accomplished by direct comparison with osteological collections that are often limited in terms of taxon sampling and number of available specimens (Bell & Mead, 2014).

Europe currently hosts only six species of geckos (Sillero et al., 2014) classified in three families: the sphaerodactylid *Euleptes europaea* (Gené, 1839), the gekkonids *Alsophylax pipiens* (Pallas, 1827), *Cyrtopodion caspium* (Eichwald, 1831), *Hemidactylus turcicus* (Linnaeus, 1758) and *Mediodactylus kotschy* (Steindachner, 1870), and the phyllodactylid *Tarentola mauritanica* (Linnaeus, 1758). A seventh species, *Tarentola fascicularis* (Daudin, 1802), occurs on the Italian islands of Lampedusa and Conigli, off the coast of Tunisia (Harris et al., 2009). Their distribution is mostly confined to Mediterranean countries, although within the territory of Europe, *A. pipiens* and *C. caspium* occur only in small areas of the southwestern part of Russia (Sillero et al., 2014).

With the goal of promoting the identification of fossil remains and skeletal remnants in owl pellets, as well as providing osteological characters useful for phylogenetic analyses, here we describe and compare the cranial osteology of the four most common and broadly distributed species of European geckos, *E. europaea*, *H. turcicus*, *M. kotschy* and *T. mauritanica*, along with a diagnostic key for the identification of their isolated skull bones. *Alsophylax pipiens*, *C. caspium* and *T. fascicularis* were excluded from our analysis because of their limited distribution in the continent, so limited that they are not included in the field guides to the European herpetofauna (among others, Arnold & Oviden, 2002; Speybroeck et al., 2016).

MATERIAL AND METHODS

The descriptions are based on 23 specimens of the aforementioned species: four specimens of *E. europaea* (MDHC 384, 388, 389); six specimens of *H. turcicus* (MDHC 26, 238 and JDD 326 – 327); five specimens of *M. kotschy* (MDHC 201, 285, 418, 419); eight specimens of *T. mauritanica* (MDHC 97, 98, 119, 194, 302; NHMW 2484, 31945). A single specimen of *Chalcides chalcides* (Linnaeus, 1758), MDHC 94, and of *Cordylus cordylus* (Linnaeus, 1758), NHMW 707, were used for comparison in the discussion related to the tooth morphology, as examples of the standard morphology of scincid and cordylid teeth respectively. All specimens are housed in the collections of the Department of Earth Sciences of the University of Turin (Massimo Delfino Herpetological Collection, MDHC), except for NHMW 707, 2484 and 31945 which are housed in the herpetological collection of the Natural History Museum of Vienna (NHMW) and JDD 326 – 327 which is housed in the personal collection of one of the authors (Juan D. Daza Herpetological Collection, JDD).

Isolated bones were photographed with a Leica M205 microscope equipped with the Leica application suite V 3.3.0 at the University of Turin and Sam Houston State University, whereas pictures of the teeth of selected specimens were taken with a Jeol JSM-IT300LV at the University of Turin. Specimens stored at the NHMW were photographed with a camera Canon EOS 50D mounted on a Leica M420 microscope.

High-resolution x-ray computed tomography of four specimens (*E. europaea* MCZ R-4463, *H. turcicus* TNHC 85380, *M. kotschy* CAS 101566 and *T. mauritanica* CAS 87112) was conducted at the University of Texas at Austin (Digimorph) using a ZEISS Xradia high-resolution X-ray computed tomographic (X-ray CT) scanner. Three dimensional models of the cranium and jaw were generated using Avizo Lite 9.0.0 (Visualization Sciences Group). The skull was digitally disarticulated from the cervical vertebrae and the jaw was also rendered separated to facilitate visibility of bones. Stack images, scanning parameters, and a 3D surface rendering for each species are available from Morphosource (<http://morphosource.org>).

The terminology used in the description of the skull bones comes mainly from Evans (2008), but when appropriate terms were not provided in this work we have adopted certain terms from Daza et al. (2008), Bell, Evans & Maisano (2003) and Barahona (1996). Names of the structures composing the tooth crown follow the terminology proposed by Kosma (2004). Bones were described following the order of Evans (2008).

Except for Figs. 1-4, the bones are figured in standard anatomical orientation. This means that when a bone is shown in dorsal or ventral views, the anterior end is above, whereas in the case of anterior or posterior views the dorsal side is above. In lateral views, the anterior end is either on the left or on the right side of the bone, depending on the bone being left or right respectively (or being viewed from the left or right side in the case of unpaired elements). It is the opposite in medial views. In Figs. 1-4, the anterior end is on the left, except for the medial, ventral and dorsal views of the dentary, in which the anterior end is on the right.

Some skeletal elements of MDHC 119 and 194 (*Tarentola mauritanica*) show a sort of osseous swelling, maybe because of some kind of pathology. This presumably pathological condition was not considered as taxonomically diagnostic and is not described in detail here, given that our comparative study was intended to deal only with the general osteology of the four species considered.

RESULTS

DESCRIPTION OF ARTICULATED SPECIMENS

Skull anatomy of the four European geckos is heterogeneous (Figs. 1-4). These species also vary in size, smallest to largest using are organized in this order: *Euleptes europaea* (10.32 mm, MCZ R-4463; Fig. 1), *Mediodactylus kotschy* (13.97 mm, CAS 101566; Fig. 3), *Tarentola mauritanica* (15.83 mm, CAS 87112; Fig. 4), and *Hemidactylus turcicus* (17.17 mm, TNHC 85380; Fig. 2).

None of the European geckos has fused nasals or parietals. The surface of the skulls of *E. europaea* and *M. kotschy* are smooth, lacking any dermal sculpturing, whereas *H. turcicus* has some scattered

pits with rough surface. The CT-scan specimen of *T. mauritanica* has deep grooves, although this might represent some artifact of the rendering given that these grooves were not observed in the skeletonised specimens. *Euleptes europaea* has two distinct mediolaterally oriented elongated (slot-like) furrows on the posterior portion of the frontal bone. The ascending nasal process of the premaxilla is narrowest and longest in *M. kotschyi*. The nasals have parallel margins and are nearly trapezoidal in all geckos except *H. turcicus*, in which the lateral margins diverge posterolaterally, resulting in an expanded posterior margin. Only in *E. europaea* do the nasals establish a contact with the prefrontals, where the prefrontal is considerably less overlapped by the facial process of the maxilla. In other geckos, the facial process separates the nasal from the prefrontal. The suborbital fenestra is large and D-shaped in *E. europaea*, whereas in the other species it is oval and reduced. A D-shaped suborbital fenestra was described in other miniaturised sphaerodactylids (Daza et al., 2008). The frontal bone forms an anterior wedge (a roughly triangular structure) in all European geckos, with variable acuteness of the medial process, and in *E. europaea* and *H. turcicus* it has two distinct anterolateral processes, these processes being small in *M. kotschyi* and absent in *T. mauritanica* (see also the description of the isolated frontal below). In all species the frontoparietal suture is nearly transverse. The parietals cover and approach the occiput more closely in the smallest species (*E. europaea*), where they likewise do not converge in a single medial process posteriorly, but rather give rise to paired posteromedial processes that cover the common crus. The pyriform recess is notably reduced in *H. turcicus* because the palatines approach each other. In all European geckos the palatine-pterygoid joint is strongly reduced, but in *E. europaea*, these two bones only interact with each other at the joint, because the palatines have an oblique posterolateral edge, contrary to the other geckos in which the palatine runs parallel to the pterygoid for a longer distance. The basipterygoid process of the sphenoid is expanded in all the European geckos, but in *E. europaea*, the expansion is minimal.

All European geckos have a tall coronoid eminence, which is unexpected, especially in the case of *E. europaea*, which differs from the condition of a reduced coronoid eminence seen in other

miniaturised sphaerodactylids. In the CT-scanned specimen of *E. europaea* the anterior surangular foramen is present in the coronoid bone, and not in the surangular portion of the compound bone. There are notable differences among the individual bones of the four species studied, and these differences will be discussed in the next section.

DESCRIPTION OF ISOLATED BONES

Nasal (Fig. 5). The nasals are paired elongated bones, trapezoidal in shape, with a ventrally concave anterior portion and a straight posterior process. Those of *E. europaea*, *T. mauritanica* and of some specimens of *H. turcicus* tend to be slightly narrower anteriorly (Fig. 5A-D, G-H). The nasals of *H. turcicus* and *T. mauritanica* have a slightly concave posterior margin, whereas, in the other taxa, the posterior margin is straight. The anterior margin is concave, whereas the lateral margins of the bone tend to be straight and parallel. The anterior edge of the bone has two anteriorly directed processes: a short anterolateral process that bends antero-ventrally, and a premaxillary process that is long and straight with a shelf to support the ascending nasal process of the premaxilla. The shelf is visible on the anterior half of the medial margin. Both dorsal and ventral surfaces are smooth. A sharp and ventrally directed ridge is present along the medial margin of the nasals of *E. europaea* and *T. mauritanica* (Fig. 5B, H). In *E. europaea*, this ridge curves laterally near its posterior end, marking the medial half of the anterior margin of the articulation surface with the frontal. The latter structure cannot be recognized in *M. kotschyi* (Fig. 5F) and *T. mauritanica* (Fig. 5H), but it is clearly visible near the posterior end of the ventral surface in *E. europaea* (Fig. 5B) and *H. turcicus* (Fig. 5D): the surface is narrow and subrectangular in the former and wide and triangular in the latter.

Frontal (Fig. 6). The frontal is unpaired. It has an approximately T-like shape in dorsal view and a posterior end that is roughly twice as large as the anterior one. In dorsal view, the lateral margins are constricted in the interorbital region, and the posterior margin is slightly concave (in *M. kotschyi*; Fig. 6K) or straight (in *E. europaea*, *H. turcicus* and *T. mauritanica*; Fig. 6A, F, P). The anterior margin is W-shaped in *E. europaea* (Fig. 6A-B), V-shaped in *H. turcicus* (Fig. 6F-G) and convex or nearly straight in *M. kotschyi* (Fig. 6K-L). In *T. mauritanica* (Fig. 6P-Q), this margin is

highly variable, perhaps partly as an artifact of disarticulation (that is, the irregularities seen in some specimens might originate from minor damage occurring on disarticulated elements). As a matter of fact, it can be either straight or slightly convex, truncated and slightly irregular. There is a small, pointed medial process in *M. kotschyi* (Fig. 6K; except for MDHC 201) and of *T. mauritanica* (Fig. 6P); this medial process is more prominent in *E. europaea* (Fig. 6A). The anterolateral processes are well defined in *E. europaea* (moderately developed and pointed; Fig. 6A), *H. turcicus* (wide, triangular and well developed; Fig. 6F) and some specimens of *M. kotschyi* (little developed and pointed). The posterior margin extends laterally forming two long posterolateral processes. These two processes expands dorso-ventrally and are continued into the cristae cranii. The dorsal surface of the bone is smooth and dorsally flattened in *E. europaea*, depressed medially in the anterior third with deep furrows, flattened in the two posterior thirds and covered with a faint ornamentation made up by grooves in *H. turcicus* (Fig. 7), smooth and sometimes slightly concave along the median axis of the bone in *M. kotschyi* and *T. mauritanica*. The articulation facets for the nasals are not bordered by ridges; they are triangular and correspond to the dorsal surface of the lateral processes in *H. turcicus* (Fig. 6F), whereas they are subrectangular and placed along the anterior margin in *E. europaea* (Fig. 6A), *M. kotschyi* (Fig. 6K) and *T. mauritanica* (Fig. 6P). Two shallow but distinct sulci are visible on the dorsal surface of the frontal of *E. europaea* (Fig. 6A) running along the lateral margin in the posterior third of the bone (Daza et al., 2014; also visible, but less marked in the fossil gecko *Gerandogekko aranbourgi*). The articulation facets with maxillae and prefrontals are visible on the anterior half of the lateral margins. They are wider in *H. turcicus* (Fig. 6H) and *T. mauritanica* (Fig. 6R) than in *E. europaea* (Fig. 6C) and *M. kotschyi* (Fig. 6M). The articulation facet with the anterior process of the postorbitofrontal is not clearly defined on the lateral margins of the posterior portion in *E. europaea* (Fig. 6C) and some specimens of *M. kotschyi* (although these are well-defined in MDHC 418 and 419). The facet for the postorbitofrontal is on the other hand visible in *H. turcicus* (Fig. 6H) and *T. mauritanica* (Fig. 6R). When both articulation surfaces with prefrontals and postorbitofrontals are visible, they are distinctly distant from one

another. The cristae cranii are projected ventrally, extending from the lateral margins of the frontal. In the midline of the bone, in ventral view, they fuse into the frontal ridge, which forms a tubular structure that is slightly flattened ventrally and encloses the olfactory tracts of the brain. The tube is subelliptical in anterior view and subcircular in posterior view. The anteroventral portion of the crista cranii has two processes; there is also another anteriorly directed process between these two processes. This middle process is well defined in *E. europaea* (Fig. 6B), *M. kotschyi* (Fig. 6L) and *T. mauritanica* (Fig. 6Q), but reduced to a small peg in *H. turcicus* (Fig. 6G). It is pointed, except for that of *T. mauritanica*, which is slightly concave anteriorly (Fig. 6Q). Comparing the middle process with the anterior process of the cristae cranii, these are subequal in length in *E. europaea* (Fig. 6C) and *T. mauritanica* (Fig. 6R), the anterior ones are longer than the middle one in *H. turcicus* (Fig. 6H), and the middle one is longer than the anterior ones in *M. kotschyi* (Fig. 6M). The anterior processes are moderately developed and define, together with the anterior margin of the crista, two anteriorly concave (slightly concave in *T. mauritanica*) surfaces with a roughly dewdrop-like shape in anterior view and a slight inclination in ventro-medial direction. Those of *E. europaea* are slightly more developed and roughly pointed in ventral view. In *H. turcicus*, moreover, the anterior processes are developed by the anterior margin and so they do not originate the concave surfaces, although their antero-dorsal surface exhibits a drop-like shape in anterior view. In *H. turcicus*, a low ridge separates the areas corresponding to the articulation surfaces with the nasals from the rest of the ventral surface of the shelf of the frontal (Fig. 6G). In *M. kotschyi*, in place of this low ridge there is a slight osseous swelling and a low ridge runs medially behind it without continuing inside the tube (Fig. 6L). In *T. mauritanica*, the median ridge is slightly more developed and a robust osseous swelling is present medially between the ridge and the medial process (Fig. 6Q). *Euleptes europaea* can show a condition similar to either that of *H. turcicus* (MDHC 388 and 389; Fig. 6B) or to that of *T. mauritanica* (MDHC 384, the largest specimen). Maximum length of the frontal of examined specimens is given in Table 1.

[Table 1]

Parietal (Fig. 8). Parietals are rectangular and paired. These bones are composed by a straight shelf, with an anterolateral process and ventrally curved postparietal processes. The lateral and posterior margins are thickened. In *E. europaea* (Fig. 8A-B) and *T. mauritanica* (Fig. 8J-K), the postero-medial corner of the bone terminates with a squared end, whereas in *M. kotschy* (Fig. 8G-H) and *H. turcicus* (Fig. 8D-E) the parietal may have either a pointed or squared end. The anterolateral process is short, without considerable anterior projection, and slightly expanded ventrally (strongly expanded in *T. mauritanica*; Fig. 8J-K). This process is well-defined in *M. kotschy* (like a short horn; Fig. 8G-H), peg-like in *E. europaea* (Fig. 8A-B), broad and flat in *H. turcicus* (Fig. 8D-E) and very short in *T. mauritanica* (Fig. 8J-K). Medially to those of *H. turcicus* and *M. kotschy* there is a small notch, which is moderately wide and shallow in *H. turcicus* (Fig. 8D-E) and more developed in *M. kotschy* (Fig. 8G-H). A thin osseous lamina forms the lateral margin of the bone from the base of the anterolateral process to the beginning of the postparietal process. This lamina provides attachment for the jaw adductor muscles. It is developed laterally and, in *M. kotschy* (Fig. 8I), also slightly dorsally. The lamina is narrow in *E. europaea* (Fig. 8A), moderately developed in *M. kotschy* (Fig. 8G), moderately to well developed in *T. mauritanica* (Fig. 8J) and prominent in *H. turcicus* (Fig. 8D). The medial margin of the parietals is generally straight and shows some interlocking wedges in *T. mauritanica* (Fig. 8J-K); in one specimen, MDHC 302, the parietal experience the fusion of these wedges in the posterior portion. The postparietal process is narrow and distally pointed. It shows different degrees of posteroventral curvature, ranging from having a mild curvature (nearly horizontal) in two specimens of *M. kotschy* (MDHC 201 and 285; Fig. 8I) to be strongly curved in *T. mauritanica* (Fig. 8L). An oblique ridge runs on the posterior margin of the parietal, by the base of the postparietal process, marking the attachment surface for the longissimus capitis neck muscles (Al Hassawi, 2007). This ridge is well marked in all the species except *E. europaea*. Around the mid-length of the lateral margin, on the ventral surface, the triangular and

small epipterygoid process (descensus parietalis process) develops in ventral direction. The process of *E. europaea* (Fig. 8C) and *T. mauritanica* (Fig. 8L) continues with a lamina that reaches the anterior margin. The one of *E. europaea* is rounded and not triangular. Medial to the process, is a shallow groove, which also continues anteriorly and posteriorly along the lateral margin. In *E. europaea* and *H. turcicus*, only a short portion of this groove is clearly recognizable near the anterior margin of the shelf. The dorsal surface of the shelf is smooth, except for that of *H. turcicus*, which shows a faint ornamentation made up of shallow grooves (Figs. 7, 8E). The ventral surface forms two shallow concavities: a larger, sub-circular one located anteriorly and a smaller and subtriangular posterior one. The anterior concavity is twice as large as the posterior one. These ventral concavities are only weakly distinguishable in *E. europaea*. Maximum length and maximum width of the parietal of examined specimens is given in Table 1.

Premaxilla (Fig. 9). The premaxilla is unpaired and formed by a ventral alveolar plate, from which the medially located ascending nasal process projects posterodorsally. The dorsal margin of the alveolar plate extends posteriorly forming a subtrapezoidal lamina. The palatal processes vary in size and extension and may appear divided medially by a notch, which is wide in all species but *E. europaea* (Fig. 9B, D). The lamina is short in *E. europaea*, but long in the other species. There is no incisive process. In some specimens of *T. mauritanica* (MDHC 119, 194 and 302), a foramen can be seen in ventral view in the middle of the lamina. The alveolar margin of the alveolar plate bears the pleurodont teeth. The ascending nasal process is long, narrow (particularly in *T. mauritanica*) with a pointed end, except in *M. kotschyi* where it has a blunt end (when disarticulated; Fig. 9K-L, N-O). The process is wider proximally in most of the species (not in *M. kotschyi*), especially in *E. europaea*. In most specimens of *M. kotschyi* (except for MDHC 418) it tends to be spatulated. In *E. europaea*, the process is more robust and shows a slight constriction by the base, taking an arrow-like shape in anterior view (Fig. 9A, E). The septonasal crest of *E. europaea* (Fig. 9E) and *T. mauritanica* (Fig. 9T) runs along the entire posterior surface of the nasal process; it is low in the former and moderately developed in the latter. In *H. turcicus* (Fig. 9J) and *M. kotschyi* (Fig. 9O), on

the other hand, the septonasal crest is small and is not extending into the end of the process. The two foramina of the longitudinal canals open by the sides of the ascending nasal process, by its junction with the alveolar plate. The maximum length of the alveolar plate is given in Table 1.

Tooth positions counts are provided in Table 2.

Maxilla (Fig. 10, 11). The paired maxillae consist of an alveolar portion, a palatal shelf and a dorso-medially developed facial process. The alveolar portion is vertical and includes the tooth-bearing alveolar border which is intercepted by the medial palatal shelf. Teeth are present along the entire length of the bone. The anterior edge that forms the joint with the premaxilla (i.e., the anterior premaxillary process) is concave, forming the anteromedial and anterolateral processes. The anteromedial process is generally larger than the anterolateral one. It is well developed and pointed in *E. europaea* (Fig. 10A-C), small and roughly subtriangular in dorsal view in *H. turcicus* (Fig. 10D-F) and *M. kotschyi* (Fig. 10G-I) and moderately developed and anteriorly truncated or pointed in *T. mauritanica* (Fig. 10J-L). The anterolateral process is almost absent in *E. europaea* (Fig. 10A-C), small and subtriangular in *H. turcicus* (Fig. 10D-F) and *T. mauritanica* (Fig. 10J-L) and little developed or absent in *M. kotschyi* (Fig. 10G-I). The superior alveolar canal passes through the base of the facial process, opening anteriorly through the vomeronasal foramen. Posteriorly, the canal opens on the dorsal surface of the palatal shelf on the wide superior dental foramen, near the posterior end of the facial process. The vomeronasal foramen is moderately wide, except in *E. europaea*, in which it is smaller. The canal opens also on the lateral surface of the maxilla, with a variable number of ventrolateral foramina: in the examined specimens, they fluctuate from 6 to 9 in *E. europaea*, from 6 to 7 in *H. turcicus*, from 4 to 7 in *M. kotschyi* and from 4 to 7 in *T. mauritanica*. The number of these foramina can be different in the two maxillae of the same specimen. The posterior end of the bone is the elongated posterior (jugal) process, which is pointed (rounded in *E. europaea*; Fig. 10A-B) and flat on the dorsal margin. On its dorsal surface, a wide but shallow groove runs in postero-medial direction starting from the superior dental foramen. Such groove is not clearly visible in *H. turcicus*, but this species exhibits another moderately shallow

groove posteriorly to the facial process, representing the position of the ventral margin of the lacrimal foramen (Fig. 11). In *M. kotschyi*, another shallow groove, bordered dorsally by a low ridge, may be present by the base of the facial process, dorsally to the superior dental foramen; in MDHC 418, this groove is medially closed and represented only by a posteriorly open foramen. The facial process is tall and subtrapezoidal in lateral view; its length is equivalent to half the length of the entire maxilla. Its posterodorsal end is rounded in *E. europaea* (Fig. 10A-B) and presents a pointed postero-dorsal projection in the other species (Fig. 10D-E, G-H, J-K). The posterior and dorsal margins of the process are straight, whereas the anterior margin is more variable between species: it is steep and inclined anteriorly in *E. europaea* (Fig. 10A-B) and *H. turcicus* (Fig. 10D-E), steep and roughly vertical in *M. kotschyi* (Fig. 10G-H) and displays a V-shaped notch in *T. mauritanica* (Fig. 10J-K). In *E. europaea*, *M. kotschyi* and *T. mauritanica*, both medial and lateral surfaces are smooth, with only a highly variable number of flanked foramina by the base of the process, whereas in *H. turcicus* the lateral surface is covered by a faint ornamentation made up of grooves and the medial side has a wide foramen by its base and a low sigmoid-shaped ridge running near the anterior margin (Fig. 11). A small foramen is visible near the antero-dorsal corner of the facial process in *E. europaea* and *T. mauritanica*: it passes through the process, opening in a ventral direction on the lateral surface and in dorsal direction on the medial one. A similar foramen seems to be present also in some specimen of *M. kotschyi* (e.g., MDHC 201 or the right maxilla of MDHC 419), but it is shifted ventrally. The maximum length of the alveolar border is reported in Table 1, whereas the number of tooth positions is provided in Table 2.

Prefrontal (Fig. 12). The prefrontal is paired and crescent-shaped in lateral view, comprising an anteriorly concave body, the orbitonasal flange, and a large, pointed dorsal process postero-dorsally directed from the medial side of its dorsal margin. A thin, smooth laminar structure, the anterodorsal process, extends anteriorly from the dorsal margin of the orbitonasal flange and is overlapped by the facial process of the maxilla. Two ventral processes project from the orbitonasal flange: a pointed posteroventral process laterally and an orbitonasal flange projection medially. The

orbitonasal flange projection is wider and better developed than the posteroventral process, and has a subtrapezoidal shape (subtriangular in *E. europaea* and *T. mauritanica* MDHC 97 and more rounded in *T. mauritanica* MDHC 98). A small lateral projection derives from the posteroventral process. The postero-lateral surface of the orbitonasal flange is smooth in all species except for *H. turcicus*, in which it may bear a faint ornamentation made up of grooves (Fig. 7). A wide notch in between the anterodorsal and the posteroventral processes marks the dorsal and medial margins of the lacrimal foramen. The notch is deep in *H. turcicus* (Fig. 12E-H) and shallow in other species (Fig. 12A-D, I-P). The dorsal process is slender in *E. europaea* (Fig. 12A-D) and *M. kotschy* (Fig. 12I-L) and stouter in *H. turcicus* (Fig. 12E-H) and *T. mauritanica* (Fig. 12M-P).

Jugal (Fig. 13). The paired jugal is straight in lateral view and slightly sigmoid shaped in dorsal view. The anterior end is dorso-ventrally flattened, pointed and wider than the posterior, whereas the latter is narrower and more robust. In *E. europaea*, the difference between the two ends is less marked (Fig. 13A-B). In *H. turcicus*, the lateral margin of the posterior end is folded in ventral direction and gives a subcylindrical shape to the end (Fig. 13D).

Postorbitofrontal (Fig. 14A-H). Gekkotans have a single element in the posterodorsal corner of the orbit and corresponds to the paired postorbitofrontal (assumed to be resulting from by the fusion of the postfrontal and postorbital [Daza et al., 2008, but see Wise & Russell, 2010 for an alternative hypothesis]). In *E. europaea* (Fig. 14A-B), *H. turcicus* (Fig. 14C-D) and *M. kotschy* (Fig. 14E-F), it is a small V-shaped bone (roughly boomerang-shaped in *E. europaea* and *H. turcicus*), with an antero-medial (anterior process) and a postero-medial (posterior process) processes. That of *T. mauritanica* (Fig. 14G-H) differs from this morphology because of the presence of a U-shaped medial margin and of a third laterally developed process, which gives it a Y-shape. The anterior and posterior processes have the same length in *M. kotschy* (Fig. 14E-F), whereas the anterior one is longer than the posterior one in *E. europaea* (Fig. 14A-B) and shorter than the posterior one in *H. turcicus* (Fig. 14C-D) and in *T. mauritanica* (Fig. 14G-H). The anterior process is the narrowest in dorsal view and has a pointed end; its anterior (orbital) margin is slightly concave. The posterior

process, which is wider in dorsal view, has a straight lateral margin (concave in *T. mauritanica*; Fig. 14G-H); its end is pointed in *E. europaea* (Fig. 14A-B), *H. turcicus* (Fig. 14C-D) and most specimens of *M. kotschy*, more squared in *M. kotschy* MDHC 285 (Fig. 14E-F) and rounded in all specimens of *T. mauritanica* (Fig. 14G-H). In lateral view, the more robust process is the anterior one. Differences in width and thickness of the two processes are less marked in *E. europaea*. The lateral process of *T. mauritanica* is shorter than the other two processes (Fig. 14G-H); it is wide and has a pointed end. The lateral corner of the bone (the vertex of the V) is rounded in *E. europaea* (Fig. 14A-B) and *H. turcicus* (Fig. 14C-D) and pointed in *M. kotschy* (Fig. 14 E-F). Both ventral and dorsal surfaces are smooth; the dorsal one is also flattened. There is no postorbitofrontal lateral notch.

Squamosal (Fig. 14I-J). The paired squamosal is small and thin. It resembles a small rod curved at the posterior end. The anterior process is pointed, whereas the posterior one is expanded.

Quadrate (Fig. 15A-L). The paired quadrate is composed by a posteriorly curved pillar structure and by a strongly posteriorly concave conch. In anterior view, the general outline of the bone is strongly rounded laterally, giving it a roughly bean-like shape. The only exception is *E. europaea*, in which the bone is rather elongated antero-dorsally, forming a narrower conch than in other species (Fig. 15A-B). The quadrate is also rounded anteriorly in lateral view. The lamina develops laterally from the anterior margin of the pillar forming a large, deep conch, whose lateral margin is defined by the tympanic crest, a slightly expanded portion of the lamina. In *M. kotschy*, the tympanic crest is slightly thicker near the ventral end of the bone (Fig. 15G-I), whereas in the other species there are no clear differences in thickness. The ends of the pillar are represented by the cephalic condyle dorsally and by the mandibular condyle ventrally. The cephalic condyle is dorsally flattened and not significantly expanded to the sides, whereas the mandibular one is divided into two portions by a concavity. The lateral portion of the mandibular condyle is more developed than the medial one. Lateral to the cephalic condyle, the lateral lamina is scarcely ossified and has a variably wide and deep squamosal notch. The quadrate foramen pierces the lateral lamina dorsally to the mandibular

condyle; sometimes two foramina are present, whereas in some cases no opening is visible. Table 1 reports the maximum length of the quadrate in the examined specimens.

Epipterygoid (Fig. 15M). The epipterygoid is a paired rod-like bone. It is straight, thin and slightly expanded at its dorsal end.

Vomer (Fig. 16A-H). The paired vomers are dorsally concave and laminar bones, with an antero-posteriorly elongated shape. Their anterior end is tapered, whereas the posterior one is slightly wider and rounded or squared. The lateral margin of the anterior half bears a notch, marking the medial margin of the vomeronasal fenestra. This notch, however, is poorly developed and so the lateral margin is convex. The articulation surface with the palatal process of the premaxilla is clearly visible by the antero-lateral margin of the anterior end. The anterior end of the vomers of *E. europaea*, moreover, may be pierced by a teardrop-shaped notch (Fig. 16A-B). A well developed, pointed, postero-dorsally directed process as long as two thirds of the vomer is present in the middle of the lateral margin. In *E. europaea* (Fig. 16B) and *M. kotschyi* (Fig. 16F), the process is concave in the medial direction, whereas the concavity cannot be clearly seen in *H. turcicus* (Fig. 16D) and *T. mauritanica* (Fig. 16H), in which the process is notably thicker in the distal portion. The process of *E. europaea* is also wide (Fig. 16A-B). In dorsal view, the articulation surface with the vomerine process of the palatine is visible ventral to the process, bordered by low ridges both ventrally and dorsally in *E. europaea* (Fig. 16B) and *H. turcicus* (Fig. 16D) and only ventrally in *T. mauritanica* (Fig. 16H). The articulation surface is not clearly recognizable in *M. kotschyi*, in which only the dorsal ridge is visible, marking the ventral margin of the postero-dorsal process (Fig. 16F). A transverse septum (barely visible in *T. mauritanica*) divides the dorsal surface into two sunken regions: the smaller vomeronasal region anteriorly and the nasal one, twice as long as the former, posteriorly. The septum corresponds on the ventral surface to a slightly sunken transverse area (barely recognizable in *T. mauritanica*). A low longitudinal ridge is present on the dorsal surface of the vomers of *E. europaea*, running from the septum up to the articulation surface with the vomerine process of the palatine.

Septomaxilla (Fig. 16I-X). Septomaxillae are small, laminar paired bones. The body of the bone is rectangular, and elongated antero-posteriorly and ventrally concave, roofing the vomeronasal cavity. Two low ridges with irregular dorsal margins run on the dorsal surface, along the lateral and medial margins. In *E. europaea* (Fig. 16K-L) and *T. mauritanica* (Fig. 16W-X), the morphology of one of the two ridges (the lateral and the medial one, respectively) is different, being high at the posterior end and tending to sharply flatten anteriorly; in the latter species, moreover, both ridges have a regular dorsal margin. In *T. mauritanica* (Fig. 16X), the medial ridge is fused with the lamina only in the posterior half and a moderately deep groove is visible by the base of its medial surface, continuing anteriorly in the space between the unfused half of the ridge and the lamina. Such a groove is visible also in some specimen of *H. turcicus* (Fig. 16P) but not *E. europaea* (Fig. 16L), whereas in *M. kotschyi* the medial surface of the medial ridge is only concave and does not show clear grooves (Fig. 16T). On the ventral surface, an arched ridge starts from the postero-medial corner and develops in antero-lateral direction, continuing on the anterior margin of a short, laterally directed triangular process in the posterior third of the bone. This process is posteriorly concave. From the postero-lateral corner, a thin (moderately robust in *T. mauritanica*; Fig. W-X) lateral process develops in posterior direction; it is roughly as long as the lamina in *E. europaea* (Fig. 16I-L), *H. turcicus* (Fig. 16M-P) and *M. kotschyi* (Fig. 16Q-T) and longer than it in *T. mauritanica* (Fig. 16U-X). In *E. europaea* (Fig. 16I-L) and *M. kotschyi* (Fig. 16Q-T), this process is clearly hook-shaped, because of a dorsolateral curve of its posterior end; in the other two species, the hook-shape is less recognizable. At the postero-medial corner, there is another thin, pointed, posteriorly directed process, which is roughly two thirds (*H. turcicus*; Fig. 16 M-N) or one half (*E. europaea*, Fig. 16I-J, and *T. mauritanica*, Fig. 16U-V) as long as the lateral process. Only a small hint of the medial process is present in *M. kotschyi* (Fig. 16Q-R).

Palatine (Fig. 17A-H). The paired palatine comprises a thin laminar bone, the pterygoid process, and two slender, pointed and antero-ventrally developed processes, namely the vomerine and maxillary processes. These two processes develop from the antero-medial and the antero-lateral

corners of the lamina, respectively, and they define the lateral walls of the choanal duct, which is continued on the ventral surface of the lamina by a shallow trough. The vomerine process is more robust and slightly longer than the maxillary one. On the lateral surface of the maxillary process of *H. turcicus* (Fig. 17D) and *T. mauritanica* (Fig. 17H), the articulation surface with the maxilla is visible. In *E. europaea* (Fig. 17A-B) and *H. turcicus* (Fig. 17C-D), a small osseous expansion projects laterally near the base of the maxillary process, forming a small, thin, subtriangular process. Usually, *M. kotschyi* does not display this expansion (Fig. 17E-F), but sometimes a small hint of it can be present. Roughly in the same position, the palatines of *T. mauritanica* show a wide foramen not closed laterally, the margins of which are formed by osseous expansions of the lateral margin (Fig. 17G-H); this foramen could represent the interorbital foramen, otherwise not recognizable in the palatines of gekkotans. No palatine ridge or palatine teeth are present.

Pterygoid (Fig. 17I-P). The pterygoid is a paired bone with a triradiate structure, having three branches developing antero-medially (palatine process), antero-laterally (pterygoid flange) and postero-laterally (quadrate process). The palatine process is composed by a wide laminar portion and by a more robust medial margin, which is strongly concave in dorsal view. The pterygoid flange is pointed and slender; it is separated by the laminar portion of the palatine process by a moderately deep notch, the pterygoid recess. Two ridges run along the flange: a poorly distinguished one on its dorsal surface and a well-developed one on its ventral surface. The quadrate process is long, curved and strongly concave in lateral direction. In dorsal view, this process has a rounded end (truncated in *T. mauritanica*; Fig. 17O-P). The sub-circular fossa columellae is located on the dorsal surface of the quadrate process and the moderately small basiptyergoid fossa is present on the medial margin. The basiptyergoid fossa is bordered dorsally by a thin and rounded ridge that develops in dorso-medial direction. In *H. turcicus*, the fossa is shallow and is defined mostly by the ridge. Posteriorly, the basiptyergoid fossa continues in the surface for the insertion of the pterygoideus muscle, which is rather flat. A moderately to well-developed ridge is visible on the dorsal surface of the quadrate process. It is not clear if this ridge is the pterygoid ridge because it

apparently does not start from the fossa columellae. The ridge is more developed in *T. mauritanica* than in other species, whereas it is not clearly recognisable in *E. europaea*. Moreover, a small hint of a real pterygoid ridge seems to be present in *T. mauritanica*, posterior to the fossa columellae. There are no pterygoid teeth. The maximum length of the pterygoids of the examined specimens is given in Table 1.

Ectopterygoid (Fig. 17Q-X). The ectopterygoid is a small, crescent-shaped, paired bone, with two pointed ends and a medial concavity. In medial view, the posterior end (postero-medial process) is divided into two pointed lappets, which embrace the pterygoid flange of the pterygoid. The dorsal lappet is longer than the ventral one. In ventral view, the lateral margin of the anterior half of the bone (anterolateral process) comprises the articulation surface with the maxilla. In the ectopterygoid of *E. europaea*, the ventral lappet is little developed and the articulation surface with the maxilla is scarcely distinguishable (Fig. 17Q). The dorsal surface of the bone is smooth.

General features of the otooccipital region (Fig. 18, 19). The otooccipital region is the portion of the braincase composed by the fusion of sphenoid, basioccipital, prootics, supraoccipital and otooccipitals (Evans, 2008). These bones are separated in juveniles but fuse during growth (Daza et al., 2008). The region is roughly as long as it is wide and slightly dorso-ventrally compressed (more compressed in *E. europaea*; Fig. A-C). Posteriorly, supraoccipital, otooccipitals and basioccipital define the wide and subcircular (subelliptical in MDHC 201, 388 and 389) foramen magnum, whereas otooccipitals and the basioccipital compose the occipital condyle, participating equally in its composition. The occipital condyles are paired in gekkotans (Daza et al. 2008), having a clear U-shaped notch that is visible in dorsal view. Between the basioccipital and each otooccipital, there is the moderately wide and subelliptical lateral aperture for the recessus scalae tympani (i.e., the anterior portion of the metotic fissure; Evans 2008). The recessus scalae tympani has a medial opening into the cranial cavity, and a dorsomedial opening (the perilymphatic foramen) into the cochlear cavity. In contrast with other species, the occipital recess is notably wide in *E. europaea* (Fig. 18B, E). The medial opening of the recessus scalae tympani is narrow and elongated, whereas

the perilymphatic foramen is smaller (larger in *E. europaea*; Fig. 18E) and rounded. In *T. mauritanica*, the medial opening is divided into two subcircular portions, both smaller than the perilymphatic foramen. The cochlear cavity opens externally with the wide fenestra ovalis, which is located between prootics and otooccipitals. Each side of the otooccipital region shows three moderately narrow semicircular canals: the anterior one develops between the prootic and the supraoccipital, the horizontal one runs between the dorsal portion of the prootic and the base of the paraoccipital process of the otooccipital, whereas the posterior one is located between the supraoccipital and the otooccipital.

Basioccipital (Fig. 18, 19, 20A-B). The unpaired basioccipital is roughly as long as it is wide and has a subtrapezoidal shape, with six sides. Its body is dorsally concave, bearing a central cranial depression, and shows two moderately developed lateral wings. The anterior margin may be roughly straight or concave and the posterior one forms the medial third of the occipital condyle. Both the ventral and the dorsal surfaces are smooth. The sphenoccipital tubercles are present at the ends of the two lateral wings, constituting the ventral wall of the recessus scalae tympani. They are poorly developed in the ventral direction in *E. europaea* (Fig. 18B-C), moderately developed in *H. turcicus* (Fig. 18G-H) and *M. kotschy* (Fig. 19B-C) and well developed in *T. mauritanica* (Fig. 19G-H). When developed, they are subtriangular in lateral view. The posterior wall of the recessus scalae tympani is marked by the crista tuberalis. The basioccipital contacts and fuses with the sphenoid anteriorly, with the prootics antero-laterally and with the otooccipitals postero-laterally.

Sphenoid (Fig. 18, 19, 20C-D). The sphenoid (sometimes called parabasisphenoid) is an unpaired bone made up by the complete fusion of parasphenoid and basisphenoid. The body of the bone has a roughly quadrangular shape, with two antero-laterally directed basiptyergoid processes starting from the antero-lateral corners. These processes are elongated and triangle-shaped, with a narrow proximal portion that enlarges distally. The distal end is tilted medio-laterally by about 30° (roughly 45° in *E. europaea*) and is slightly dorso-laterally concave. A laminar, anteriorly directed supravenuous process is present dorsal to each basiptyergoid process: it is weakly developed in *M.*

kotschyi (Fig. 19B, D) and *H. turcicus* MDHC 26 (Fig. 18G, I), moderately developed in *T. mauritanica* (Figs. 19G, I, 20D) and well developed in *E. europaea* (Fig. 18B, D) and *H. turcicus* MDHC 238. Laterally, each supravenuous process is connected with the continuation of the crista prootica. In lateral view, supravenuous and basipterygoid processes are separated by the groove of the lateral head vein, which starts posteriorly from a small foramen. In *H. turcicus*, this groove is closed laterally and is represented only by an anteriorly opened foramen, whereas the posterior foramen is not visible in *E. europaea*. Two small and cylindrical trabeculae cranii are located between the basipterygoid processes, continuing posteriorly in two low cristae trabeculares. These cristae border the sella turcica, which includes the hypophysial fossa, laterally. They are not visible in *M. kotschyi* (Fig. 19D), whereas in other species they are low and arched, curving laterally and merging with the anterior margin of the supravenuous processes. The small trabeculae are close in *H. turcicus* (fused medially in MDHC 26; Fig. 18I) and in most specimens of *T. mauritanica* (Fig. 19I), whereas a small hint of parasphenoid rostrum (cultriform process in Daza et al. 2008) is present between them in *M. kotschyi* MDHC 285 and in *T. mauritanica* MDHC 194. In dorsal view, the sphenoid is crossed transversely by the dorsally developed crista sellaris, which marks the posterior margin of the sella turcica and continues laterally, contacting the prootics at the alar processes. The crista does not develop a dorsum sellae and therefore the sella turcica is not covered dorsally. Two abducens foramina pierce the crista antero-posteriorly. The dorsal surface of the sella turcica shows a high degree of variation: in *E. europaea*, it is always smooth (Fig. 18D); in *H. turcicus*, the only visible structures are a foramen in MDHC 26 (Fig. 18I) and a low ridge encircling a circular area in MDHC 238, both placed anteriorly to the center of the crista sellaris; in *M. kotschyi*, the surface is smooth and not separated in MDHC 201, 418 and 419, whereas in MDHC 285 the anterior half is occupied by the shallow hypophysial fossa and the posterior one is divided into two portions by a low median ridge (Fig. 1D); in *T. mauritanica*, it is smooth (MDHC 302; Fig. 20D) or it may have a low median ridge running from the trabeculae to the crista sellaris (in MDHC 194) or only a hint of a portion of such ridge (anterior portion in MDHC 119 and posterior portion

in MDHC 97 and 98; Fig. 19I). Posterior to the crista, the dorsal surface of the sphenoid is smooth. The ventral surface is also smooth, but it exhibits a depressed area in the middle: this area is shallow in *E. europaea* (Fig. 18E), *H. turcicus* (Fig. 18J) and *M. kotschyi* (Fig. 19E), but strongly deepened in *T. mauritanica* (Fig. 19J). In anterior view, medially to the base of the basipterygoid processes, one can see the anterior openings of the vidian canals, which open also medially in the sella turcica (with the internal carotid foramina) and postero-laterally in direction of the contact with the prootics. From the latter openings, the recessus vena jugularis extends postero-dorsally on both sides of the sphenoid, continuing along the anterior inferior process of the prootics. No well-developed cristae ventrolaterales (parasphenoid wings in Daza et al. 2008) can be seen posteriorly in *E. europaea*, *H. turcicus* and *M. kotschyi*, whereas two small, pointed ones are present at the posterolateral corners in *T. mauritanica* (Figs. 19J, 20C-D). The sphenoid contacts and fuses with the basioccipital posteriorly and prootics postero-laterally.

Supraoccipital (Fig. 18, 19, 20E). The unpaired supraoccipital, which includes the epiotic of Jollie (1960), has a transversely elongated shape and is posteriorly inclined. It consists of a thin medial portion and two wide lateral portions that form the roof of the cavum capsularis. The posterior margin of the bone defines the dorsal margin of the foramen magnum. There is no processus ascendens (ascendens tecti synotic process) on the anterior margin, but other structures are present. The supraoccipitals of *H. turcicus* (Fig. 18I) and *M. kotschyi* (Fig. 19D) have a pointed tubercle with a posteriorly directed point in the middle of the dorsal surface. In *H. turcicus*, the dorsal surface of this tubercle is flattened. In *T. mauritanica*, in the place of the tubercle there is a robust ridge, with the shape of an antero-posteriorly compressed W in dorsal view (Fig. 19I). The anterior surface of this ridge is smooth, whereas its dorsal margin is slightly irregular in anterior view. A low midline crest runs posteriorly from the midpoint of the ridge. The dorsal surface of the supraoccipital of *E. europaea*, on the other hand, is smooth (Fig. 18D). The dorsal portions of the anterior semicircular canals are located along the anterior margin of the bone, whereas those of the posterior ones run from the postero-lateral corners to the middle of the dorsal surface. On each side,

the canals merge in the common crus, which opens in the cavum capsularis (Fig. 20E). The common crus is recognizable externally as an osseous swelling whose lateral margin can develop a slightly laterally developed lamina. The lamina is absent in *E. europaea*, *H. turcicus* and in *T. mauritanica* MDHC 97 and 302. On the medial surface of the lateral portions of the bone, near the contact with the prootic, one can see the moderately wide and postero-dorsally opened endolymphatic foramen. The supraoccipital is fused with the prootics antero-laterally and the otooccipitals postero-laterally.

Prootic (Fig. 18, 19, 20F-G). The prootic is a paired bone comprising a posterior process posteriorly, an alar process antero-dorsally and an anterior inferior process ventrally. The posterior process is almost entirely occupied by the horizontal semicircular canal and, antero-dorsally to the latter, by the anterior semicircular canal. A short projection of the posterior end of this process covers the proximal half of the anterior surface of the paroccipital process of the otooccipital. From the antero-dorsal end of the anterior semicircular canal, the alar process develops in an antero-dorsal direction; its anterior margin, the crista alaris, bears the medio-laterally expanded articulation surface with the epipterygoid. The process is well developed and, in lateral view, it is triangular (*H. turcicus*, Fig. 18G, and *T. mauritanica*, Figs. 19G, 20F) or subtrapezoidal (*E. europaea*, Fig. 18B, and *M. kotschyi*, Fig. 19B) in shape and has a pointed (*H. turcicus*) or rounded (other species) distal end. The incisura prootica, the facial foramen and the laminar crista prootica stand out on the anterior inferior process. The incisura prootica is wide and located medio-ventrally to the alar process. Except for *T. mauritanica* MDHC 98, it is dorsally closed by an osseous expansion. The facial foramen opens both on the lateral and medial surfaces, ventral to the horizontal semicircular canal and the crista prootica. The well-developed crista prootica runs antero-ventrally starting from the ventral end of the anterior semicircular canal. It also continues on the posterior process, curving posteriorly and becoming a ridge that runs ventrally to the horizontal semicircular canal, and on the sphenoid in the supravenuous process. In *H. turcicus* and *M. kotschyi*, the anterior and posterior portions of the crista are separated by a small notch. The posterior portion of the recessus vena

jugularis runs ventrally to the crista prootica. The recessus is directed postero-dorsally and reaches the facial foramen in *M. kotschyi* (Fig. 19B), whereas in *E. europaea* (Fig. 18B), *H. turcicus* (Fig. 18G) and *T. mauritanica* (Fig. 19G) it ends ventral to the foramen without contacting it. In the latter species, the foramen is housed in a separated entocarotid fossa (not distinguishable in *M. kotschyi*), which is particularly distinct in *E. europaea*, mainly because of the presence of a laterally directed osseous expansion marking its ventral margin. In some specimens, this expansion can touch the ventral surface of the crista prootica. The prootic portion of the recessus is shallower than that of the sphenoid. In medial view, two other large foramina are visible, opening in a concave acoustic recess (Fig. 20F): the smaller anterior acoustic foramen is located dorsally to the facial foramen and opens in the ampullary recess, whereas the large posterior acoustic foramen is placed slightly posteriorly and opens internally between the cochlear cavity and the cavum capsularis. These two foramina carry the branches of the vestibulocochlear nerve. The posterior margin of the posterior acoustic foramen is marked by the otooccipital. The inner structures of the prootic, which encloses the anterior portion of the inner ear, include the anterior portions of the cavum capsularis dorsally, the cochlear cavity ventrally and the cochlear crest between them (Fig. 20G). The cavum capsularis is flanked by the opening of the anterior semicircular canal dorsally and by that of the horizontal semicircular canal laterally. Near its medio-ventral corner, there is the opening of the ampullary recess. The dorsal half of the anterior wall of the cochlear cavity houses the wide groove for the perilymphatic duct. This bone fuses with the sphenoid antero-ventrally, the basioccipital postero-ventrally, the supraoccipital postero-dorsally and the otooccipital posteriorly.

Otooccipital (Fig. 18, 19, 20H-I). The otooccipital is a paired bone made up by the fusion of exoccipital and opisthotic, which are not recognizable as separate elements. The fusion is still marked by the slit-like vagus foramen (Bever, Bell & Maisano, 2005). Each otooccipital participates in the composition of the occipital condyles, composing a third of it. In posterior view, the vertically oriented posterior semicircular canal stands out on the posterior surface of the bone, continuing dorsally on the supraoccipital. Between the ventral portion of the canal and the occipital

condyle, there are some foramina: the largest and most dorsally placed is the vagus foramen (i.e., the posterior portion of the metotic fissure; Evans 2008), whereas the others can be interpreted as hypoglossal foramina, which may be highly variable in number, even among the otooccipitals of a same specimen. 2 or 3 hypoglossal foramina are present in *E. europaea* and *M. kotschyi*, 1, 5 or 6 in *H. turcicus* and 2, 3 or 4 in *T. mauritanica*. In MDHC 119, 194, 384 (only on the right side) and 388, another foramen is visible, in posterior view, dorsal to the vagus foramen and medial to the posterior semicircular canal. The roughly rectangular paroccipital process is present laterally; it is short in *E. europaea* (Fig. 18A-E), but longer in all other species. At the base of this process, one can see the posterior portion of the horizontal semicircular canal. In *M. kotschyi* and *T. mauritanica*, a ridge (well developed in MDHC 97, 119 and 194, low in the other specimens) starts from the dorsal end of the semicircular canal and runs along the dorsal half of the anterior surface of the process, ending around the middle of its length; the proximal half of this ridge marks the contact between otooccipital and prootic. Another low ridge can be seen near the ventral margin of the same surface in all species, running along the entire process. This second ridge is only a hint in *E. europaea* and in most specimens of *T. mauritanica*, except for MDHC 119. On the lateral surface of the bone, the crista interfenestralis develops in antero-ventral direction starting from the paroccipital process; this crista marks the dorsal margin of the lateral opening of the recessus scalae tympani. The otooccipital encloses the posterior portion of the inner ear, housing the posterior walls of the cavum capsularis dorsally and of the cochlear cavity ventrally (Fig. 20H). The two cavities are not separated by ridges or grooves. The cavum capsularis is flanked by the opening of the horizontal semicircular canal laterally and by that of the posterior semicircular canal dorsally; its inner surface shows the openings of the ampullary recess ventrally and of the utricular recess dorsally. In *T. mauritanica*, a low ridge divides in two the lateral half of the cavum, starting medially between the two recesses housed in it. The cochlear cavity presents the perilymphatic foramen, which opens in the recessus scalae tympani. The medial wall of the cavity also shows the posterior margin of the

posterior acoustic foramen. The otooccipital contacts the basioccipital ventrally, the prootic anteriorly and the supraoccipital dorsally, fusing with them.

Stapes (Fig. 20J). The paired stapes is a small bone with a slender shaft and an enlarged, elliptical medial footplate. Only in *H. turcicus*, the footplate is subcircular. Near the footplate, the shaft is pierced by the moderately wide stapedia foramen.

Dentary (Fig. 21). The dentary is a long paired bone, straight in both dorsal and medial view; only the anterior end bends moderately in a medial direction. The medial surface of the anterior end is covered by the mandibular symphysis, which is narrow and inclined anteriorly of about 45°. A channel, the Meckelian fossa, is present on the medial surface of the bone and houses the anterior portion of the Meckel's cartilage. The fossa is closed in a tubular structure composed by completely fused osseous expansions of the ventral margin and the subdental ridge; it opens at the anterior end only via a small foramen, which continues anteriorly in a groove in all species except for *T.*

mauritanica, and at the posterior end by a V-shaped (U-shaped in *T. mauritanica*; Fig. 21K) notch. The notch extends along the posterior third (*E. europaea*; Fig. 21B), fourth (*H. turcicus*; Fig. 21E), fifth (*T. mauritanica*; Fig. 21K) or sixth (*M. kotschyi*; Fig. 21H) of the alveolar shelf. The tube is moderately narrow and tends to shrink anteriorly. Dorsal to the fossa, the alveolar shelf bears the teeth. The posterior end of the bone bears two posteriorly directed laminar processes: the inferior one ventrally and the superior one dorsally. The inferior process is long and pointed, whereas the superior one is smaller and divided into two pointed projections. The size of the two projections is subject to individual variation, but as a rule the dorsal one is shorter. A variable number of antero-posteriorly aligned mental foramina is present on the lateral surface of the dentary, which is otherwise smooth. Dentaries of *E. europaea* show 5 to 8 mental foramina, those of *H. turcicus* 5 to 6, those of *M. kotschyi* 4 to 5 and those of *T. mauritanica* 3 to 5. The ventral margin of the bone is straight in medial view. Maximum length of the alveolar shelf is shown in Table 1.

Splénial (Fig. 22A-H). The paired splénial is a reduced, thin, blade-like bone. It is pierced by two foramina: the anterior inferior foramen antero-dorsally and the anterior mylohyoid foramen postero-

ventrally. These foramina are located on the anterior portion of the bone; they are both wide, but, in *M. kotschyi* and *T. mauritanica* (except for NHMW 31945), the anterior mylohyoid foramen is represented only by a notch on the ventral margin (Fig. 22E-H). The posterior corner of the splenial of *E. europaea* (Fig. 22A-B) and *H. turcicus* (Fig. 22C-D) expands posteriorly and bends laterally, forming a long, thin, pointed process, which contributes to form the ventral surface of the lower jaw. In *M. kotschyi* (Fig. 22E-F), this bone takes part only in the formation of the medial surface, whereas in *T. mauritanica* only a small triangular process derived from the lateral bending of the posterior end is present (Fig. 22G-H). Both medial and lateral surfaces are otherwise smooth.

Coronoid (Fig. 22I-X). The paired coronoid has an irregular shape, with four processes. In dorsal view, it is strongly crescent-shaped. In the middle, it shows the dorsally developed coronoid process, which is thin and roughly pointed (dorsally rounded in *E. europaea*; Fig. 22K-L). The other processes are the labial process (anterolaterally), the anteromedial process (anteromedially) and the posteromedial process (posteriorly). Both the anteromedial and the labial processes are pointed, but the former is always larger and longer than the latter. Moreover, the anteromedial process is composed by two laminae split by a groove in dorsal view; the medial lamina is smaller than the lateral one. The splitting is almost not recognizable in *E. europaea*. A foramen pierces the center of the lateral lamina of the process. The posteromedial process is moderately long, thin and pointed (in *H. turcicus*, Fig. 22M-P, and *M. kotschyi*, Fig. 22Q-T) or rounded (in *E. europaea*, Fig. 22I-L, and *T. mauritanica*, Fig. 22U-X) in dorsal view. A well-developed osseous lamina is present between this process and the coronoid one

Compound bone (Fig. 23). A paired compound bone, composed by the fusion of the surangular, articular, prearticular and angular, is present in adult gekkotans. Only in young individuals, it can be still separated in two portions (angular/surangular and prearticular/articular). The presence of an angular in the mandible of most gekkotans is doubted by Jollie (1960), but the same author says also that it could be fused with prearticular and surangular. The compound bone is straight in medial view and encloses the posterior portion of the Meckel's cartilage in a tubular cavity. Its

anterior end is pointed. Dorsally to the second fourth of the bone, there is an expanded area with a slightly irregular and slightly sunken medio-dorsal surface, bordered postero-dorsally by an arched ridge. The development of the ridge is highly variable in *T. mauritanica*: it is absent in MDHC 98, barely visible in MDHC 97 and 194 and well developed in MDHC 119 and 302. In medial view, the narrow and antero-posteriorly elongated adductor fossa stands out by the third fourth of the bone. Posterior to the fossa, the articular condyle which contacts the quadrate, is subcircular, postero-medially directed, inclined posteriorly of about 45° and divided into two sunken areas by a medially located swelling. The wide and dorso-medially concave retroarticular process develops posteriorly from the ventral margin of the condyle; it consists of a thin, posteriorly truncated osseous lamina. In *M. kotschyi*, the posterior portion of the lamina tends to expand, forming a lobe in medial view (Fig. 23G-H). In *E. europaea* (Fig. 23A-B), *H. turcicus* (Fig. 23D-E) and *T. mauritanica* (Fig. 23J-K), the process is only slightly larger posteriorly and so it has a subrectangular shape rather than a lobed one. A low longitudinal lateral crest is present in the middle of the lateral surface of the process, except for *E. europaea* (Fig. 23B), whereas a foramen for the chorda tympani is always present on the medial surface, near its antero-ventral corner. The lateral surface of the compound bone is smooth, except for the presence of two foramina: the anterior surangular foramen, located near the dorsal margin by the anterior expanded area, and the posterior surangular foramen, located anteriorly to the articulation condyle, in the middle of the surface. In *E. europaea* (Fig. 23B) and *T. mauritanica* (Fig. 23K), the posterior surangular foramen is shifted towards the dorsal margin of the bone and opens in dorsal direction. In the latter species, moreover, a short ridge is present on the dorsal margin, between the foramen and the condyle (Fig. 23K). There is no angular process.

DENTITION

All four species have a homodont dentition, made up by closely spaced, pleurodont, cylindrical and slender teeth (Fig. 24A-D). Teeth are present only on premaxillae, maxillae and dentaries; there are no palatine or vomerine teeth. With the only exception of *T. mauritanica*, teeth are slightly larger at their base and narrow towards a slightly pointed tip. Narrowing is not visible in the aforementioned

species, whose tip is as wide as the rest of the tooth and rather rounded in medial view. The number of tooth positions for the studied specimens is given in Table 2. The tooth crown is always bicuspid, although wear sometimes makes it difficult to recognize this condition. Two parallel and slightly lingually tilted cutting edges are recognizable, running antero-posteriorly and divided by a moderately deep antrum intercristatum. The antrum is moderately wide by the tip of the tooth, but narrows towards the anterior and posterior corners of the crown. This narrowing is particularly distinct in *H. turcicus* (Fig. 24B), whereas it is not present in the teeth of *T. mauritanica* (Fig. 24D), whose antrum appears also to be wider than the one of the other species. The cutting edges do not touch each other in any of the species. The lateral (labial) edge comprises the crista mesialis anteriorly and the crista distalis posteriorly, which meet at the top of the tooth in the cuspis labialis. The medial (lingual) edge, on the other hand, is made up by the crista lingualis anterior anteriorly and the crista lingualis posterior posteriorly, meeting in the middle in the cuspis lingualis. The medial edge appears to be less prominent in *T. mauritanica* than in other species (Fig. 24D). A low carina intercuspidalis seems to be visible in some teeth (see, for example, MDHC 201; Fig. 24C), connecting transversely the cuspis lingualis with the cuspis labialis. This carina, however, is often not visible, either because of a real absence or because of tooth wear. In medial view, the lateral edge is located dorsally compared to the medial one. Neither an angulus medialis nor an angulus distalis are clearly recognizable by the end of the cristae with the same name, given that their passage into the related culmen lateris is rather indistinct. Striae are visible neither on the labial nor on the lingual surfaces of the crown.

[Table 2]

DISCUSSION

SKULL BONES

Skull bones of European gekkotans display features that are typical of geckos in general, such as: small and subrectangular nasals; unpaired frontal with fused cristae cranii; paired and laterally expanded parietals; absence of parietal foramen; absence of parietal fossa; reduced jugal; presence of a single, small and Y- or V-shaped bone clasping the frontoparietal suture, herein termed postorbitofrontal (following Daza et al., 2008, and Daza & Bauer, 2010); reduced squamosal lacking a dorsal process; absence of a medial lamina on the quadrate; presence of a squamosal notch on the quadrate; presence of a contact between epipterygoid and prootic; absence of palatal teeth; absence of a vertical pterygoid flange; presence of a distinct groove for the lateral head vein on each side of the sphenoid; absence of a developed parasphenoid rostrum; absence of the processus ascendens of the supraoccipital; alar process of the prootic well developed; incisura prootica anterodorsally closed; stapedia foramen piercing the stapes; Meckelian fossa closed in a tubular structure; and coronoid provided with a labial process (Estes, 1983; Evans, 2008).

As is common in gekkotans (Evans, 2008), skull bones of the European species are lightly built. This is mainly due to the high number of bones reduced or lost in these lizards, which produce loss of many skull sutures (lack of postorbital bar by reduction of circumorbital bones), loss of supratemporal bar due to a reduction of postorbitofrontal and squamosal, and a simplified post-temporal bar. In some forms a reduction of terminal ossification in adults produces paedomorphic traits (e.g. unfused premaxillae, parietals, and nasals in some groups). The highest degree of robustness is found in *T. mauritanica*, which is also the largest one of the four species (Speybroeck et al., 2016). Another common gekkotan feature is the unornamented external surface of dermal bones (Evans, 2008). The presence of ornamented skeletal elements was reported only in a few genera, whereas most geckos have smooth bones. This is also the case of three out of four species of European geckos, with the light ornamentation of *H. turcicus* as the only exception. In other geckos with ornamented skull, this condition is originated by co-ossification of dermal bone and skin during the life of the animal, starting from a completely unornamented skull in neonates and resulting in the presence of ornamentation in adults (Bauer, 1990). All examined specimens of *H.*

turcicus show ornamented skull bones, but some kind of variation in the development of the ornamentation seems to be present in this species also, as evidenced by the fact that it can be either present or absent on the prefrontals. Future studies including newly unclosed individuals may help to clarify if the pattern of variation in *H. turcicus* is similar to the one of other ornamented gekkotans.

At the anterior end of the frontal, the presence of projections extending anteriorly under the nasals (i.e., medial and lateral process) and their development are clearly variable features among the species studied herein. In fact, they are consistently present only in *E. europaea* (both medial and lateral ones, even though the latter are less developed) and *H. turcicus* (only the well-developed lateral ones), although poorly developed processes may also be present in the other species. When present, these processes increase the complexity of the articulation with the nasals, and consequently its stiffness. Whether this may have a distinct functional significance or not is not clear. European geckos have highly kinetic skulls (Mezzasalma et al., 2014), but the fronto-nasal contact is not one of the main joints involved in cranial kinesis.

Euleptes europaea and *H. turcicus* display peculiar features in their maxillae too. The main difference of those of *E. europaea* is the facial process lacking projections, implying a missing contact between the maxilla and the frontal. Unlike those of the other species, on the other hand, maxillae of *H. turcicus* are distinctly marked by a groove for the lacrimal foramen. In all species, this foramen is marked medially and dorsally by the prefrontal, ventrally by the maxilla and the jugal, and laterally by the maxilla. The foramen of *E. europaea*, *M. kotschy* and *T. mauritanica*, however, appears to be narrower compared to that of *H. turcicus*, as evidenced by the shallower notch on the prefrontal in the former three species. This enlargement of the foramen could also be the cause of the mark on the maxilla. *Hemidactylus turcicus* also displays a ridge on the medial surface of the facial process, which is absent in all other European geckos. A medial ridge, carina maxillaris (sensu Müller, 1996), is also present in the maxillae of some lacertids and teiids (Müller, 2002; Evans, 2008), giving attachment to the connective tissue that separates the nasal sac

(dorsally) from the nasolacrimal duct (ventrally). However, this carina is arched rather than sigmoid and is located more posteriorly if compared to the one of *H. turcicus*. These differences in shape and location cast some doubt on their possible homology.

Because of the medial closure of the Meckelian fossa of the dentary, gekkotans have a strongly reduced splenial. Evans (2008) and Daza et al. (2008) report that this bone is sometimes absent (e.g., *Pristurus*, *Ptyodactylus* and all “sphaerodactyls” sensu Daza et al., 2008), but the finding of a small free splenial in a young *Ptyodactylus* led El-Toubi & Kamal (1962) to hypothesize that, at least in this genus, it fuses with the dentary during ontogeny. In a posterior interpretation, Daza and Bauer (2012) hypothesized that the splenial fuses to the coronoid in sphaerodactyls and *Pristurus*, this observation is supported by the irregular shape of the lingual process of the coronoid, which develops a feet-like structure. When present, the splenial of geckos can partly replace the angular in forming the ventral surface of the lower jaw (Jollie, 1960; Evans, 2008). All the European gekkotans studied herein have a free splenial, but only in *E. europaea* and *H. turcicus* does this bone appreciably replace the angular. Whether the ventral surface of the lower jaw is completed by an angular fused in the compound bone or by a combination of fused prearticular and surangular cannot be clearly stated without a focused embryological study, but we herein follow Daza et al. (2008: 1355) in considering that the angular is probably present and fused with the rest of the compound bone.

DENTITION

The described tooth morphology (pleurodont teeth provided with two parallel, longitudinal and slightly lingually bending cutting edges separated by a groove-like space) matches perfectly with the standard gekkotan morphology reported by Sumida & Murphy (1987) and recalls also the F morphotype of Kosma (2004), which is widespread in cordylids, gerrhosaurids and scincids and rarely present in lacertids, teiids and xantusiids. Similar bicuspid teeth with parallel longitudinal edges are also reported for scincids of the genus *Chalcides* by Caputo (2004) and for *Scincella lateralis* by Townsend et al. (1999). The absence of striations, however, clearly distinguishes

gekkotan teeth from those of most representatives of the latter families. Moreover, at least in scincids and cordylids, the crown is distinctly more curved in lingual direction than it is in gekkotans (Fig. 24E-F).

In contrast with the classical view of a completely homogeneous dentition composed by simple, monocuspid and cylindrical teeth (among others, Kluge, 1967; Bailon, 1991; Delfino, 2004; Bolet & Evans, 2013), a certain degree of variation is present among the studied species, as already pointed out for non-European species by Sumida & Murphy (1987). Even if *H. turcicus* also presents its own peculiar feature (i.e., the strong narrowing of the antrum intercristatum towards the corners), the main differences are shown by *T. mauritanica*, whose teeth have a larger and more rounded crown, a notably large antrum intercristatum and a less developed medial cutting edge. According to Sumida & Murphy (1987), a low or even absent medial edge is a feature shared by a number of large gekkotans (e.g., *Gekko gecko*, *Gekko vittatus*). Due to the fact that *T. mauritanica* is the largest one among the species we have considered, it is possible that this difference is linked to size, rather than having a real phylogenetic or functional significance. More difficult to fathom is the significance of the wider antrum: this could be a size-related trait too, but a different explanation cannot be excluded a priori. It should be noted, though, that all four species feed on essentially the same groups of arthropods (Gil, Guerrero & Perez-Mellado, 1994; Saenz, 1996; Hódar et al., 2006) and therefore a functional relevance is maybe unlikely. The same holds true for the narrow antrum of *H. turcicus*. No significant difference is present between the teeth of *E. europaea* and *M. kotschy*. Because these two species belong to different families, have different sizes (the former is much smaller than the latter) and their diet is similar and comparable to those of the other species, this affinity could be due simply to the maintenance of a primitive condition of the whole Gekkota group.

As for the number of teeth carried by each tooth-bearing bone, it seems that the largest species, *T. mauritanica*, has also a greater number of teeth on both maxillae and dentaries, on average. This could suggest a possible link between this feature and the size of the animal. However, it is

interesting to note that the greatest number of dentary tooth positions (37) was not found on a representative of this species, but in *M. kotschyi* MDHC 285, a medium-sized taxon. The number of premaxillary tooth positions, on the other hand, seems to be comparable throughout the four species; the only possible exception is *E. europaea*, which seems to have a lower number of teeth. From a morphofunctional point of view, tooth crowns with two parallel cutting edges composed by two cristae meeting in an apex were usually associated with a better capability of grasping and controlling preys in an insectivorous diet (Sumida & Murphy, 1987; Townsend et al., 1999; Caputo, 2004). This agrees with the arthropod-based diet of European gekkotans.

DIAGNOSTIC KEY

Squamosal, epipterygoid and stapes are not included in the following key because according to our results they lack significant interspecific differences. Because of it being a variable feature that can lead to wrong conclusions (for example, the identification of the bones of juveniles of larger species as those of adults of smaller ones), size is not considered in the key. However, it can still be a useful tool in case of absence of diagnostic differences (e.g., quadrates of *H. turcicus* and *T. mauritanica*), taking also into account that a juvenile condition may be recognised in some skeletal elements thanks to the possible presence of juvenile features (see, for example, Evans, 2008).

Nasal

- 1. Articulation surface with the frontal recognisable.....2
- Articulation surface with the frontal not recognisable.....3
- 2. Articulation surface with the frontal narrow and subrectangular.....*E. europaea*
- Articulation surface with the frontal wide and triangular.....*H. turcicus*
- 3. Presence of a ventral osseous expansion along the medial margin.....*T. mauritanica*
- Absence of the ventral osseous expansion.....*M. kotschyi*

Frontal

- 1. Presence of a faint ornamentation made up by grooves on the dorsal surface and of large and triangular lateral processes.....*H. turcicus*

- Dorsal surface not ornamented and lateral processes absent or little developed.....2

2. Presence of a well-developed medial process and of lateral grooves on the posterior portion of the dorsal surface.....*E. europaea*

- Absence of lateral grooves; medial process absent or little developed...*M. kotschy*/*T. mauritanica*

Parietal

1. Lateral lamina well developed; dorsal surface ornamented.....*H. turcicus*

- Lateral lamina less developed; dorsal surface not ornamented.....2

2. Lateral lamina low; groove near the lateral margin visible only by the anterior

margin.....*E. europaea*

- Lateral lamina moderately or well developed; groove near the lateral margin clearly visible both anteriorly and posteriorly to the epipterygoid process.....3

3. Presence of an anterior laminar development of the epipterygoid process; postparietal process strongly curved in ventral direction.....*T. mauritanica*

- Absence of anterior laminar development of the epipterygoid process; postparietal process less curved ventrally, sometimes straight in lateral view.....*M. kotschy*

Premaxilla

1. Ascending nasal process robust and arrow-shaped.....*E. europaea*

- Ascending nasal process narrow and not arrow-shaped.....2

2. Septonasal crest moderately developed for the entire length of the ascending nasal

process.....*T. mauritanica*

- Septonasal crest low developed, not reaching the distal tip of the ascending nasal process.....3

3. Ascending nasal process proximally wider and with a pointed distal tip.....*H. turcicus*

- Ascending nasal process not proximally wider and spatulate.....*M. kotschy*

Maxilla

1. Facial process provided with a faint ornamentation made up by grooves on the lateral surface and a sigmoid ridge on the medial one; presence of the groove of the lacrimal foramen.....*H. turcicus*

- Both lateral and medial surfaces of the facial process smooth; absence of the groove of the lacrimal foramen.....2

2. Posterior process rounded posteriorly; dorsal end of facial process rounded, without projections.....*E. europaea*

- Posterior process pointed posteriorly; dorsal end of facial process provided with a postero-dorsal projection.....3

3. Anteromedial and anterolateral process small or even absent; anterior margin of the facial process vertical.....*M. kotschyi*

- Anteromedial process moderately developed; presence of a V-shaped notch on the anterior margin of the facial process.....*T. mauritanica*

Prefrontal

1. Postero-lateral surface of the orbitonasal flange possibly provided with a faint ornamentation made up of grooves; notch of the lacrimal foramen deep.....*H. turcicus*

- Postero-lateral surface of the orbitonasal flange smooth; notch of the lacrimal foramen shallow.....2

2. Dorsal process stocky.....*T. mauritanica*

- Dorsal process slender.....*E. europaea, M. kotschyi*

Jugal

1. Posterior end folded.....*H. turcicus*

- Posterior end not folded.....2

2. Anterior end distinctly wider than the posterior one.....*M. kotschyi/T. mauritanica*

- Difference in width between anterior and posterior ends less marked.....*E. europaea*

Postorbitofrontal

1. Y-shaped, with a lateral process.....*T. mauritanica*

- V-shaped, without lateral process.....2

2. Lateral corner pointed.....*M. kotschyi*

- Lateral corner rounded.....3

3. Anterior process longer than the posterior one.....*E. europaea*

- Anterior process shorter than the posterior one.....*H. turcicus*

Quadrate

1. Rather straight in anterior view.....*E. europaea*

- Strongly laterally rounded (bean shaped) in anterior view.....2

2. Tympanic crest slightly thicker ventrally.....*M. kotschy*

- No clear differences in the thickness of the tympanic crest.....*H. turcicus/T. mauritanica*

Vomer

1. Postero-lateral process medially concave.....2

- Postero-lateral process not concave and strongly thickened distally.....3

2. Postero-lateral process wide; articulation surface with vomerine process of the palatine visible.....*E. europaea*

- Postero-lateral process narrow; articulation surface with the vomerine process of the palatine not recognisable.....*M. kotschy*

3. Articulation surface with the vomerine process of the palatine bordered by ridges both dorsally and ventrally.....*H. turcicus*

- Articulation surface with the palatine bordered by a ridge only ventrally.....*T. mauritanica*

Septomaxilla

1. Lateral process not hook-shaped.....2

- Lateral process hook-shaped.....3

2. Posterior portion of the medial ridge low.....*H. turcicus*

- Posterior portion of the medial ridge high.....*T. mauritanica*

3. Medial process long.....*E. europaea*

- Medial process short.....*M. kotschy*

Palatine

- 1. Articulation surface with the maxilla on the maxillary process not recognisable.....2
- Articulation surface with the maxilla on the maxillary process recognisable.....3
- 2. Presence of a small triangular osseous expansion on the lateral margin.....*E. europaea*
- Lateral margin without osseous expansions or, if present, expansion reduced to a small hint.....*M. kotschyi*
- 3. Lateral margin with a simple triangular osseous expansion.....*H. turcicus*
- Lateral margin with a wide and laterally open foramen.....*T. mauritanica*

Pterygoid

- 1. Posterior end of the quadrate process truncated in dorsal view.....*T. mauritanica*
- Posterior end of the quadrate process rounded in dorsal view.....2
- 2. Basipterygoid fossa shallow.....*H. turcicus*
- Basipterygoid fossa moderately deep.....3
- 3. Dorsal ridge on the quadrate process recognisable.....*M. kotschyi*
- Dorsal ridge on the quadrate process not recognisable.....*E. europaea*

Ectopterygoid

- 1. Ventral lappet of the posteromedial process little developed; articulation surface with the maxilla scarcely distinguishable.....*E. europaea*
- Ventral lappet moderately developed; articulation surface with the maxilla distinct.....other species

General features of the otooccipital region

- 1. Medial opening of the recessus scalae tympani divided into two portions.....*T. mauritanica*
- Medial opening of the recessus scalae tympani undivided.....2
- 2. Recessus scalae tympani and related lateral opening wide.....*E. europaea*
- Recessus scalae tympani and related lateral opening narrow.....*H. turcicus/M. kotschyi*

Basioccipital

- 1. Sphenoccipital tubercles poorly developed.....*E. europaea*

- Sphenooccipital tubercles moderately developed.....*H. turcicus*/*M. kotschyi*
- Sphenooccipital tubercles well developed.....*T. mauritanica*

Sphenoid

1. Groove of the lateral head vein enclosed in a canal.....*H. turcicus*
 - Groove of the lateral head vein laterally open.....2
2. Sunken area on the ventral surface deep; presence of small cristae ventrolaterales...*T. mauritanica*
 - Sunken area on the ventral surface shallow; absence of cristae ventrolaterales.....3
3. Cristae trabeculares low but visible.....*E. europaea*
 - Cristae trabeculares not distinguishable.....*M. kotschyi*

Supraoccipital

1. Absence of structures on the dorsal surface.....*E. europaea*
 - Presence of structures on the dorsal surface.....2
2. Presence of a W-shaped ridge.....*T. mauritanica*
 - Presence of a pointed tubercle.....3
3. Dorsal surface of the tubercle flat.....*H. turcicus*
 - Dorsal surface of the tubercle not flat.....*M. kotschyi*

Prootic

1. Alar process triangular in lateral view.....2
 - Alar process subtrapezoidal in lateral view.....3
2. Distal end of the alar process pointed.....*H. turcicus*
 - Distal end of the alar process rounded.....*T. mauritanica*
3. Recessus vena jugularis ending ventrally to the facial foramen; entocarotid fossa distinct.....*E. europaea*
 - Recessus vena jugularis reaching facial foramen; entocarotid fossa not distinguishable.....*M. kotschyi*

Otooccipital

- 1. Paroccipital process short.....*E. europaea*
- Paroccipital process long.....2
- 2. Absence of ridges on the dorsal half of the anterior surface of the paroccipital process.....*H. turcicus*
- Presence of a ridge on the dorsal half of the anterior surface of the paroccipital process.....3
- 3. Lateral half of the cavum capsularis undivided.....*M. kotschy*
- Lateral half of the cavum capsularis divided by a ridge.....*T. mauritanica*

Dentary

- 1. Absence of groove by the anterior end; posterior notch of the Meckelian fossa U-shaped.....*T. mauritanica*
- Presence of a groove by the anterior end; posterior notch V-shaped.....2
- 2. Posterior notch of the Meckelian fossa extending on the posterior third of the alveolar shelf.....*E. europaea*
- Posterior notch of the Meckelian fossa extending on the posterior fourth of the alveolar shelf.....*H. turcicus*
- Posterior notch of the Meckelian fossa extending on the posterior sixth of the alveolar shelf.....*M. kotschy*

Splénial

- 1. Posterior corner not bending laterally.....*M. kotschy*
- Posterior corner bending laterally.....2
- 2. Presence of a long posterior process.....*E. europaea/H. turcicus*
- Absence of a long posterior process.....*T. mauritanica*

Coronoid

- 1. Dorsal tip of the coronoid process rounded.....*E. europaea*
- Dorsal tip of the coronoid process pointed.....2
- 2. Distal end of the posteromedial process pointed.....*H. turcicus/M. kotschy*

- Distal end of the posteromedial process rounded.....*T. mauritanica*

Compound bone

1. Retroarticular process lobe-shaped.....*M. kotschyi*

- Retroarticular process subrectangular.....2

2. Absence of a longitudinal lateral crest on the retroarticular process.....*E. europaea*

- Presence of a low longitudinal lateral crest on the retroarticular process.....3

3. Posterior surangular foramen located in the middle of the lateral surface; absence of a ridge on the dorsal margin of the posterior end.....*H. turcicus*

- Posterior surangular foramen shifted dorsally; presence of a ridge on the dorsal margin of the posterior end.....*T. mauritanica*

Dentition

1. Tooth crown as wide as tooth base.....*T. mauritanica*

- Tooth crown narrower than tooth base.....2

2. Narrowing of the antrum intercristatum notably distinct.....*H. turcicus*

- Narrowing of the antrum intercristatum less distinct.....*E. europaea/M. kotschyi*

CONCLUSIONS

European gekkotans have a lightly-built skull comprising bones that show the major features of typical gecko skulls. However, significant differences are displayed by almost every bone (being squamosal, epipterygoid and stapes the only exceptions), leading to the definition of a detailed diagnostic key, which will be useful to identify isolated skeletal elements. This key could then be used in future studies dealing either with fossil remains of geckos or with the dietary habits of animals that prey on these lizards.

The comparative analysis herein carried out has also pointed out other interesting features, such as the differences in the development of the processes present on the anterior margin of the frontal, the peculiar morphological features of the maxillae of *E. europaea* and *H. turcicus* and the slightly

different tooth morphology. Deeper studies are needed in order to better understand the morphofunctional or phylogenetical significance of these features, if any.

Moreover, it is shown that *H. turcicus* can be included among the geckos provided with ornamented dermal skull bones, even though its ornamentation is faint if compared with other ornamented genera. Anyway, the degree of ornamentation appears to be subject to some kind of intraspecific variation, which could be better understood only with dedicated studies including complete ontogenetic series.

REFERENCES

Al Hassawi AM. 2007. *A comparative anatomy of the neck region in lizards: a research study.* Bloomington, Indiana: Trafford Publishing.

Arnold EN. 1989. Towards a phylogeny and biogeography of the Lacertidae: relationships within an Old-World family of lizards derived from morphology. *Bulletin of the British Museum of Natural History, Zoology* **55**: 209–257.

Arnold EN, Arribas O, Carranza S. 2007. Systematics of the Palearctic and Oriental lizard tribe Lacertini (Squamata: Lacertidae: Lacertinae), with descriptions of eight new genera. *Zootaxa* **1430**: 1–86.

Arnold N, Oviden D. 2002. *A field guide to the reptiles and amphibians of Britain and Europe.* London: Harper Collins Publisher.

Autumn K, Sitti M, Liang YA, Peattie AM, Hansen WR, Sponberg S, Kenny TW, Fearing R, Israelachvili JN, Full RJ. 2002. Evidence for van der Waals adhesion in gecko setae. *Proceedings of the national Academy of Sciences of the United States* **99**: 12252–12256.

Bailon S. 1991. Amphibiens et reptiles du Pliocène et du Quaternaire de France et d'Espagne: mise en place et évolution des faunes. Unpublished Ph.D. Thesis, University of Paris VII.

Barahona FF. 1996. Osteología craneal de lacértidos de la Península Ibérica e Islas Canarias: análisis sistemático filogenético. Unpublished D. Phil Thesis, Universidad Autónoma de Madrid.

- Barahona F, Barbadillo LJ. 1997.** Identification of some Iberian lacertids using skull characters. *Revista Española de Herpetología* **11**: 47–62.
- Barahona F, Barbadillo LJ. 1998.** Inter- and intraspecific variation in the post-natal skull of some lacertid lizards. *Journal of Zoology* **245**: 393–405.
- Bauer A.M. 1990.** Phylogenetic systematics and biogeography of the Carphodactylini (Reptilia, Gekkonidae). *Bonner Zoologische Monographien* **30**: 1–217.
- Bauer AM. 2013.** *Geckos: The animal answer guide*. Baltimore, Maryland: The John Hopkins University Press.
- Bell CJ, Mead JI. 2014.** Not enough skeletons in the closet: collections-based anatomical research in an age of conservation conscience. *The Anatomical Record* **297**: 344–348.
- Bell CJ, Evans SE, Maisano JA. 2003.** The skull of the gymnophthalmid lizard *Neusticurus eupleopus* (Reptilia: Squamata). *Zoological Journal of the Linnean Society* **139**: 283–304.
- Bever GS, Bell CJ, Maisano JA. 2005.** The ossified braincase and cephalic osteoderms of *Shinisaurus crocodilurus* (Squamata, Shinisauridae). *Palaeontologia Electronica* **8**: 4A.
- Blain H-A. 2009.** Contribution de la paléoherpétofaune (Amphibia & Squamata) à la connaissance de l'évolution du climat et du paysage du Pliocène supérieur au Pléistocène moyen d'Espagne. *Treballs del Museu de Geologia de Barcelona* **16**: 39–170.
- Bolet A, Evans SE. 2013.** Lizards and amphisbaenians (Reptilia, Squamata) from the late Eocene of Sossís (Catalonia, Spain). *Palaeontologia Electronica* **16**: 8A.
- Caputo V. 2004.** The cranial osteology and dentition in the scincid lizards of the genus *Chalcides* (Reptilia, Scincidae). *Italian Journal of Zoology* **71**: 35–45.
- Čerňanský A, Klembara J, Smith KT. 2016.** Fossil lizard from central Europe resolves the origin of large body size and herbivory in giant Canary Island lacertids. *Zoological Journal of the Linnean Society* **176**: 861–877.

- Čerňanský A, Smith KT. 2017.** Eolacertidae: a new extinct clade of lizards from the Palaeogene; with comments on the origin of the dominant European reptile group – Lacertidae. *Historical Biology*: 1-21.
- Daudin F.M. 1802.** *Histoire naturelle, générale et particulière des reptiles; ouvrage faisant suit à l'histoire naturelle générale et particulière, composée par Leclerc de Buffon; et rédigée par C.S. Sonnini, membre de plusieurs sociétés savants.* Paris: F. Dufart.
- Davis WK. 1974.** The Mediterranean gecko, *Hemidactylus turcicus* in Texas. *Journal of Herpetology* **8**: 77–80.
- Daza JD, Abdala V, Thomas R, Bauer AM. 2008.** Skull anatomy of the miniaturized gecko *Sphaerodactylus roosevelti* (Squamata: Gekkota). *Journal of Morphology* **269**: 1340–1364.
- Daza JD, Bauer AM. 2010.** The circumorbital bones of the Gekkota (Reptilia: Squamata). *The Anatomical Record* **293**: 402–413.
- Daza JD, Bauer AM. 2012.** A new amber-embedded sphaerodactyl gecko from Hispaniola, with comments on morphological synapomorphies of the Sphaerodactylidae. *Breviora* **529**: 1–28.
- Daza JD, Bauer AM, Snively ED. 2014.** On the fossil record of the gekkota. *The Anatomical Record* **297**: 433–462.
- Daza JD, Herrera A, Thomas R, Claudio HJ. 2009.** Are you what you eat? A geometric morphometric analysis of gekkotan skull shape. *Biological Journal of the Linnean Society* **97**: 677–707.
- Delfino M. 2004.** The Middle Pleistocene herpetofauna of Valdemino Cave (Liguria, North-Western Italy). *Herpetological Journal* **14**: 113–128.
- Eichwald E. 1831.** *Zoologia specialis, quam expositis animalibus tum vivis, tum fossilibus potissimum rossiae in universum, et poloniae in specie, in usum lectionum publicarum in Universitate Caesarea Vilnensi.* Vilnius: Zawadski.
- El-Toubi MR, Kamal AM. 1962.** The development of the skull of *Ptyodactylus hasselquistii*. III, The osteocranium of a late embryo. *Journal of Morphology* **108**: 193–201.

- Estes R. 1983.** *Handbuch der Paläoherpetologie 10A. Sauria terrestria, Amphisbaenia.* München: Friedrich Pfeil.
- Evans SE. 2008.** The skull of lizards and tuatara. In: Gans C, Gaunt A, eds. *Biology of the Reptilia.* Ithaca, New York: Society for the Study of Amphibians and Reptiles, 1–347.
- Ficalbi E. 1882.** *Lo scheletro di un geko. Osteologia del platidattilo mauritanico come sinossi delle osteologia dei gechidi.* Pisa: T. Nistri.
- Gamble T, Greenbaum E., Russell AP, Jackman TR, Bauer AM. 2012.** Repeated origin and loss of toepads in geckos. *PLoS ONE* **7**: e39429.
- Gamble T, Greenbaum E, Jackman TR, Bauer AM. 2015.** Into the light: diurnality has evolved multiple times in geckos. *Biological Journal of the Linnean Society* **115**: 896–910.
- Gené J. 1839.** Synopsis reptilium Sardiniae indigenorum. *Memorie della Reale Accademia delle Scienze di Torino* **1**: 257–285.
- Gil MJ, Guerrero F, Perez-Mellado V. 1994.** Seasonal variation in diet composition and prey selection in the Mediterranean gecko *Tarentola mauritanica*. *Israel Journal of Zoology* **40**: 61–74.
- Harris DJ, Carretero MA, Corti C, Lo Cascio P. 2009.** Genetic affinities of *Tarentola mauritanica* (Reptilia: Gekkonidae) from Lampedusa and Congli islet (SW Italy). *North-Western Journal of Zoology* **5**: 197–205.
- Hódar JA, Pleguezuelos JM, Villafranca C, Fernández-Cardenete JR. 2006.** Foraging mode of the Moorish gecko *Tarentola mauritanica* in an arid environment: inferences from abiotic setting, prey availability and dietary composition. *Journal of Arid Environments* **65**: 83–93.
- Howard JG, Parmerlee Jr. JS. 2001.** Natural history of the edficarian geckos *Hemidactylus mabouia*, *Thecadactylus rapicauda*, and *Sphaerodactylus sputator* on Anguilla. *Caribbean Journal of Science* **37**: 285–288.
- Jollie MT. 1960.** The head skeleton of the lizard. *Acta Zoologica* **41**: 1–64.
- Kamal AM. 1961.** The chondrocranium of *Hemidactylus turcica*. *Anatomischer Anzeiger* **109**: 89–108.

- Kamal AM. 1965.** Observations on the chondrocranium of *Tarentola mauritanica*. *Proceedings of the Egyptian Academy of Sciences* **19**: 1–9.
- Klemmer K. 1957.** Untersuchungen zur osteologie und taxionomie der europäischen mauereidechsen. *Abhandlungen der Senckenbergischen Naturforschenden Gesellschaft* **496**: 1–56.
- Kosma R. 2004.** The dentitions of recent and fossil scincomorphan lizards (Lacertilia, Squamata) – Systematics, functional morphology, paleocology. Unpublished D. Phil. Thesis, Universität Hannover.
- Klembara J, Dobiašová K, Hain M, Yaryhin O. 2017.** Skull anatomy and ontogeny of legless lizard *Pseudopus apodus* (Pallas, 1775): heterochronic influences on form. *The Anatomical Record* **300**: 460–502.
- Klembara J, Hain M, Dobiašová K. 2014.** Comparative anatomy of the lower jaw and dentition of *Pseudopus apodus* and the interrelationships of species of subfamily Anguinae (Anguimorpha, Anguinae). *The Anatomical Record* **297**: 516–544.
- Klembara J, Rummel M. 2016.** New material of *Ophisaurus*, *Anguis* and *Pseudopus* (Squamata, Anguinae, Anguinae) from the Miocene of the Czech Republic and Germany and systematic revision and palaeobiogeography of the Cenozoic Anguinae. *Geological Magazine*: 1–25.
- Kluge A. 1967.** Higher taxonomic categories of gekkonid lizards and their evolution. *Bulletin of the American Museum of Natural History* **135**: 1–59.
- Linnaeus C. 1758.** *Systema naturæ per regna tria naturæ, secundum classes, ordines, genera, species, cum characteribus, differentiis, synonymis, locis. Tomus I. Editio decima, reformata.* Stockholm: Laurentii Salvii.
- Mezzasalma M, Maio N, Guarino FM. 2014.** To move or not to move: cranial joints in european gekkotans and lacertids, an osteological and histological perspective. *The Anatomical Record* **297**: 463–472.
- Müller J. 1996.** Eine neue art der echten eidechsen (Reptilia: Lacertilia: Lacertidae) aus dem Unteren Miozän von Poncenat, Frankreich. *Mainzer Geowissenschaftliche Mitteilungen* **25**: 79–88.

- Müller J. 2002.** Skull osteology of *Parvilacerta parva*, a small-sized lacertid lizard from Asia Minor. *Journal of Morphology* **253**: 43–50.
- Newbery B, Jones DN. 2007.** Presence of Asian House Gecko *Hemidactylus frenatus* across an urban gradient in Brisbane: influence of habitat and potential for impact on native gecko species. In: Lunney D, Eby P, Hutchings P, Burgin S, eds. Pest or Guest: the zoology of overabundance. Mosman Australia: Royal Zoological Society of New South Wales, 59–65.
- Pallas PS. 1827.** *Zoographia Rosso-Asiatica, sistens omnium animalium in extenso imperio rossico et adjacentibus maribus observatorum recensioem, domicilia, mores et descriptiones, anatomen atque icones plurimorum. Vol. 3.* St. Petersburg: Caesarea Academie Scientiarum.
- Rieppel O. 1984.** The structure of the skull and jaw adductor musculature in the Gekkota, with comments on the phylogenetic relationships of the Xantusiidae (Reptilia: Lacertilia). *Zoological Journal of the Linnean Society* **82**: 291–318.
- Röll B. 2001.** Multiple origin of diurnality in geckos: evidence from eye lens crystallins. *Die Naturwissenschaften* **88**: 293–296.
- Roulin A, Dubey S. 2012.** The occurrence of reptiles in Barn Owl diet in Europe. *Bird Study* **59**: 504–508.
- Russell AP. 2002.** Integrative functional morphology of the gekkotan adhesive system (Reptilia: Gekkota). *Integrative and Comparative Biology* **42**: 1154–1163.
- Saenz D. 1996.** Dietary overview of *Hemidactylus turcicus* with possible implications of food partitioning. *Journal of Herpetology* **30**: 461–466.
- Sillero N, Campos J, Bonardi A, Corti C, Creemers R, Crochet P-A, Crnobrnja Isailović J, Denoël M, Ficetola GF, Gonçalves J, Kuzmin S, Lymberakis P, de Pous P, Rodríguez A, Sindaco R, Speybroeck J, Toxopeus B, Vieites DR, Vences M. 2014.** Updated distribution and biogeography of amphibians and reptiles of Europe. *Amphibia-Reptilia* **35**: 1–31.
- Speybroeck J, Beukema W, Bok B, Van Der Voort J, Velikov I. 2016.** *Field guide to the amphibians and reptiles of Britain and Europe.* London & New York: Bloomsbury.

- Steindachner F. 1870.** Herpetologische Notizen (II). Reptilien gesammelt Während einer Reise in Sengambien. *Sitzungsberichte der Kaiserlichen Akademie der Wissenschaften in Wien* **62**: 326–348.
- Sumida SS, Murphy RW. 1987.** Form and function of the tooth crown structure in gekkonid lizards (Reptilia, Squamata, Gekkonidae). *Canadian Journal of Zoology* **65**: 2886–2892.
- Townsend VRJr, Akin JA, Felgenhauer BE, Dauphine J, Kidder SA. 1999.** Dentition of the ground skink, *Scincella lateralis* (Sauria, Scincidae). *Copeia* **1999**: 783–788.
- Uetz P, Hošek J, editors. 2016.** The Reptile Database, <http://www.reptile-database.org>, accessed April 25, 2016.
- Vickaryous MK, Meldrum G, Russell AP. 2015.** Armored geckos: a histological investigation of osteoderm development in *Tarentola* (Phyllodactylidae) and *Gekko* (Gekkonidae) with comments on their regeneration and inferred function. *Journal of Morphology* **276**: 1345–1357.
- Villa A, Georgalis GL, Tschopp E, Delfino M. 2017.** Osteology, fossil record and palaeodiversity of the European lizards. *Amphibia-Reptilia* **38**: 79–88.
- Vitt LJ, Caldwell JP. 2009.** *Herpetology. An Introductory Biology of Amphibians and Reptiles - Third Edition*. Burlington, Massachusetts, U.S.A.: Academic Press.
- Wellborn V. 1933.** Vergleichende osteologische Untersuchungen an Geckoniden, Eublephariden und Uroplatiden. *Sitzungsberichte der Gesellschaft der naturforschender Freunde zu Berlin* **1933**: 126–199.
- Wise PA, Russell AP. 2010.** Development of the dorsal circumorbital bones in the leopard gecko (*Eublepharis macularius*) and its bearing on the homology of these elements in the gekkota. *The Anatomical Record* **293**: 2001–2006.

FIGURE CAPTIONS

Figure 1. *Euleptes europaea* (MCZ R-4463). A-C: skull in dorsal (A), ventral (B) and left lateral (C) views. D-G: lower jaw in lateral (D), medial (E), ventral (F) and dorsal (G) views.

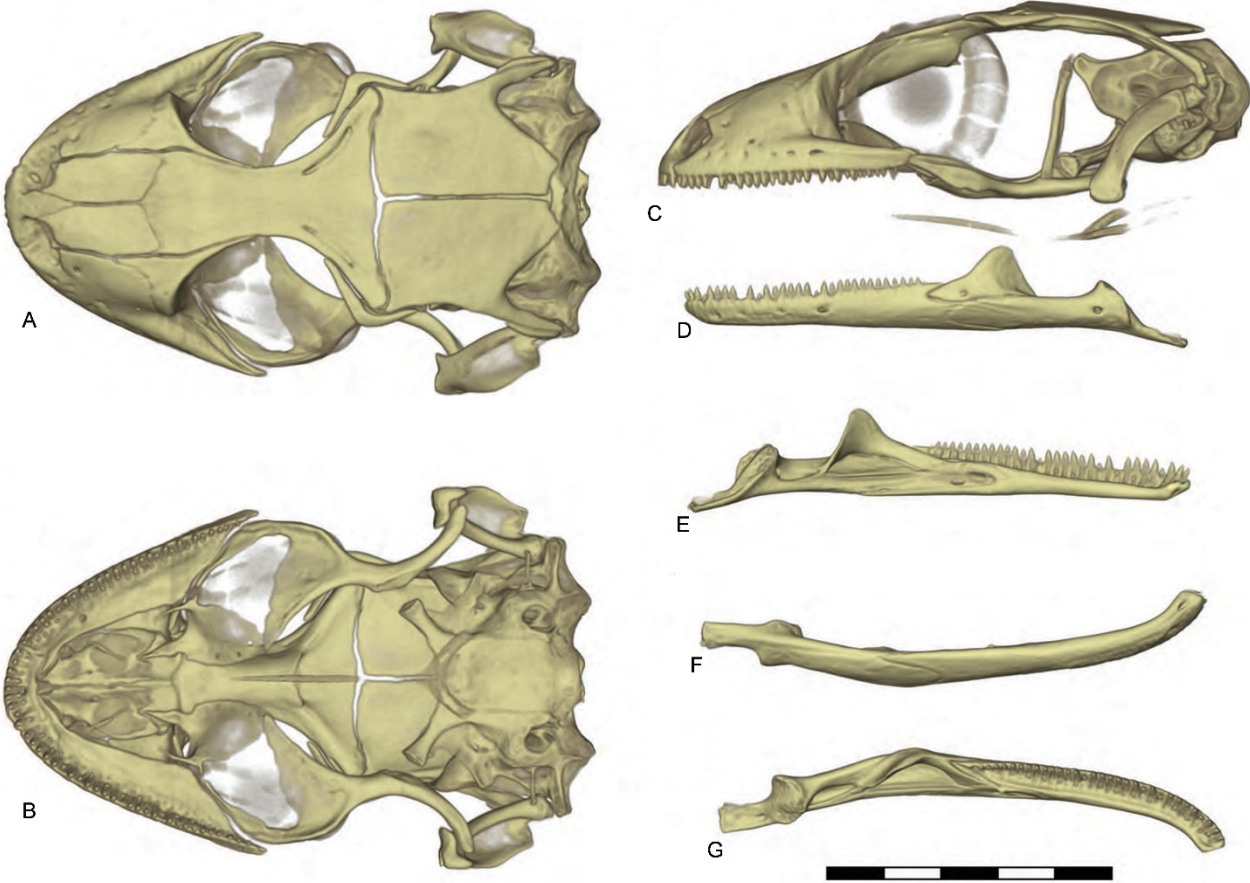


Figure 2. *Hemidactylus turcicus* (TNHC 85380). A-C: skull in dorsal (A), ventral (B) and left lateral (C) views. D-G: lower jaw in lateral (D), medial (E), ventral (F) and dorsal (G) views.

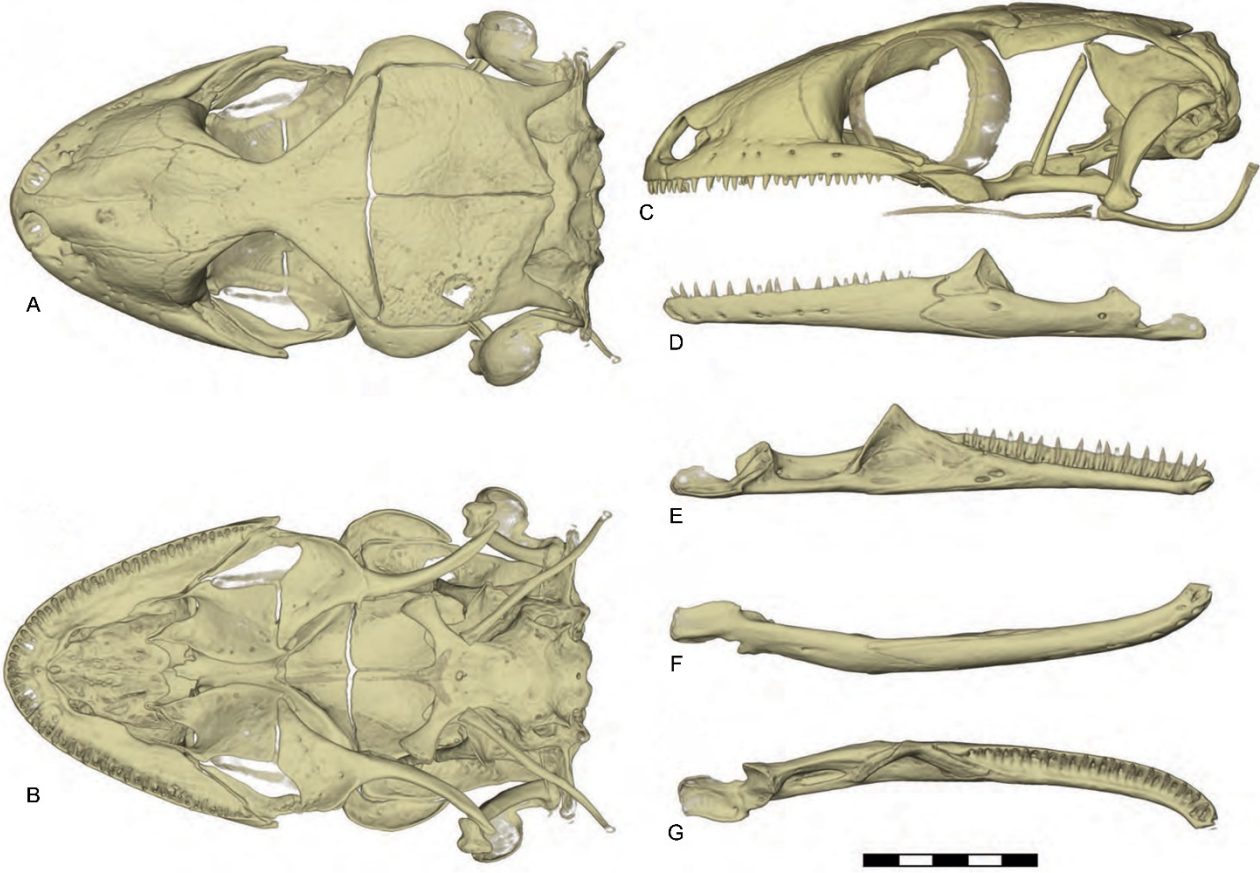


Figure 3. *Mediodactylus kotschyi* (CAS 101566). A-C: skull in dorsal (A), ventral (B) and left lateral (C) views. D-G: lower jaw in lateral (D), medial (E), ventral (F) and dorsal (G) views.

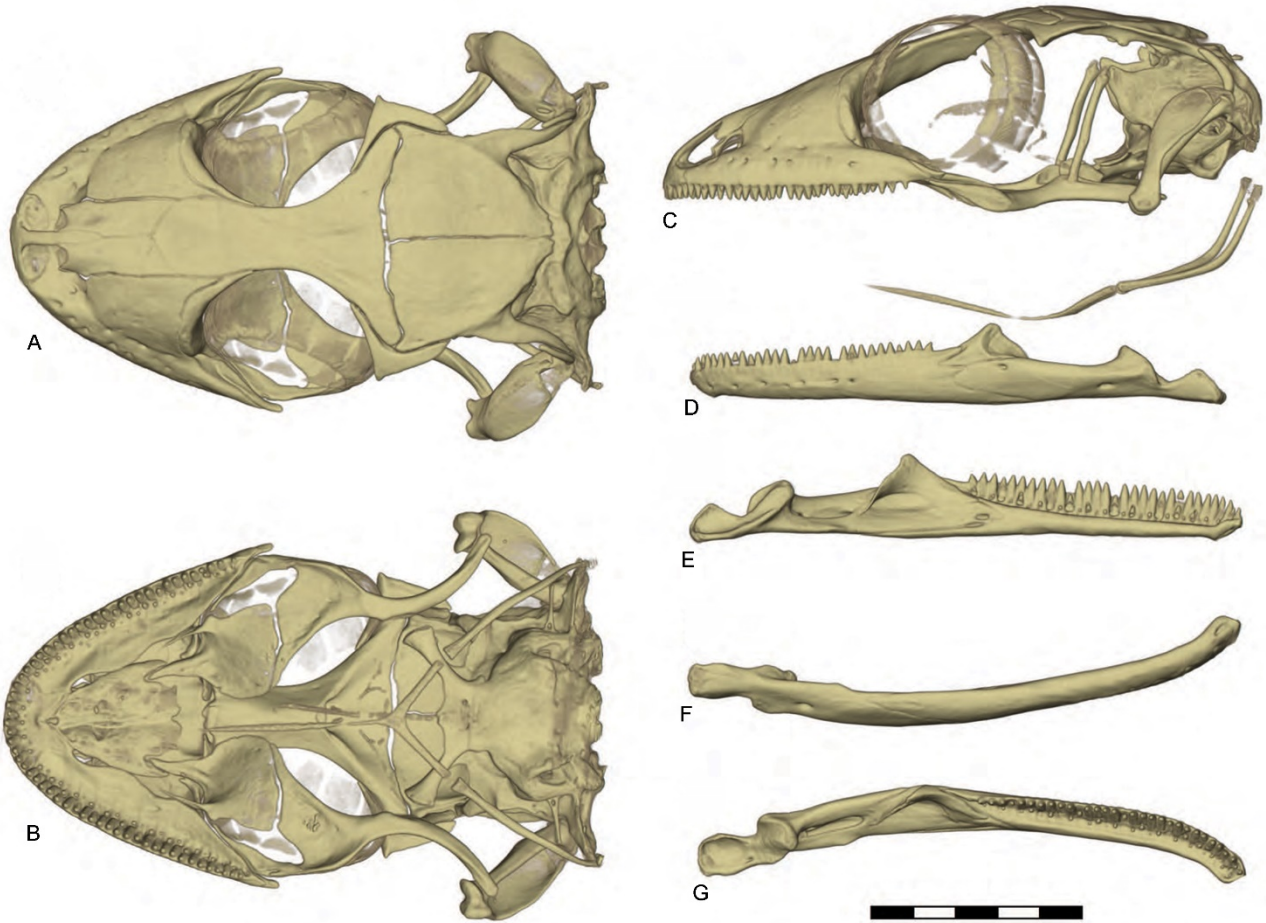


Figure 4. *Tarentola mauritanica* (CAS 87112). A: osteoderm cover. B-D: skull in dorsal (B), ventral (C) and left lateral (D) views. E-H: lower jaw in lateral (E), medial (F), ventral (G) and dorsal (H) views.

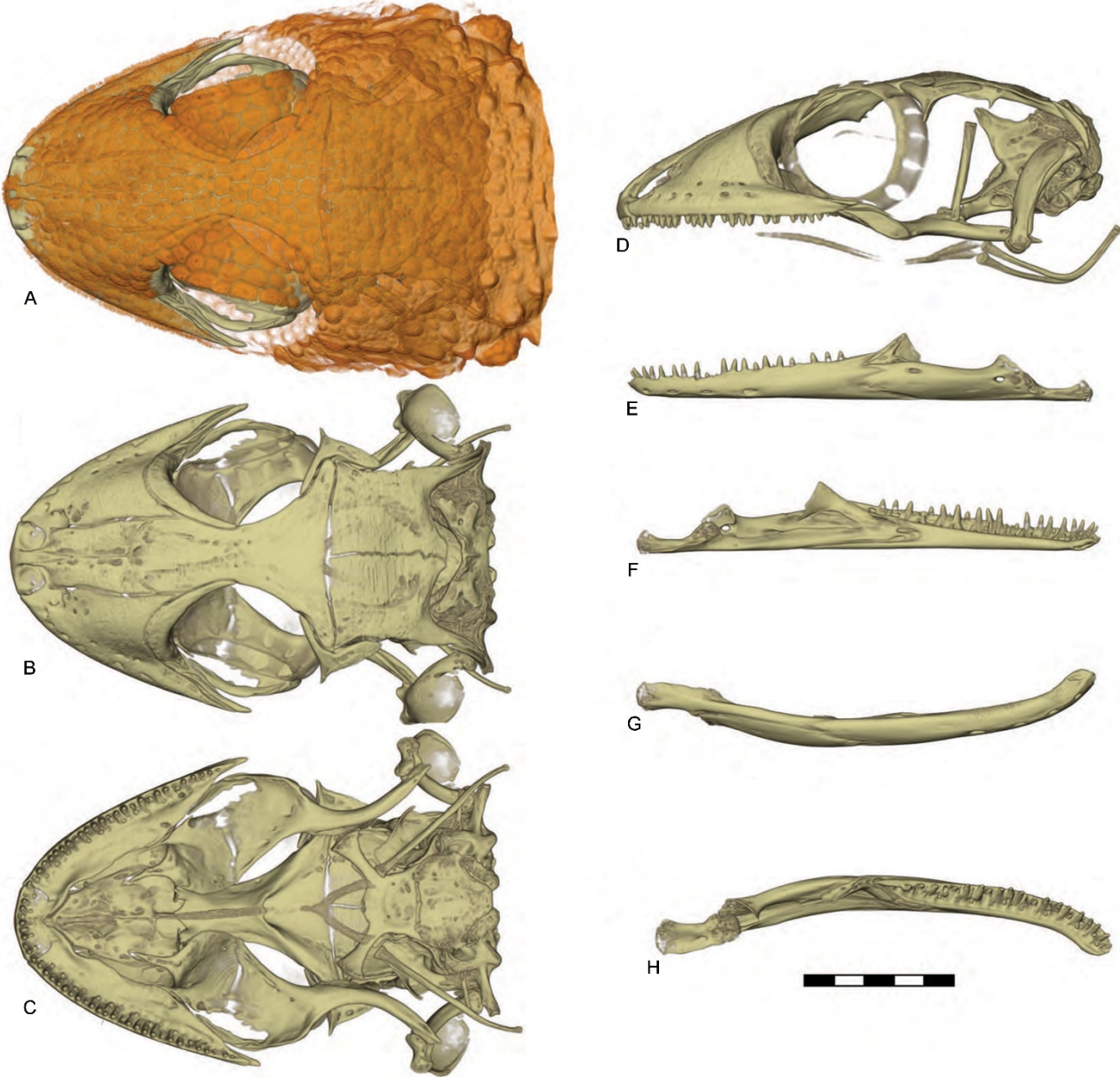


Figure 5. A-B: *E. europaea* (MDHC 389), left nasal in dorsal (A) and ventral (B) views. C-D: *H. turcicus* (MDHC 238), left nasal in dorsal (C) and ventral (D) views. E-F: *M. kotschyi* (MDHC 285), right nasal in dorsal (E) and ventral (F) views. G-H: *T. mauritanica* (MDHC 302), left nasal in dorsal (G) and ventral (H) views. The arrows mark important diagnostic structures. Abbreviations: alp, anterolateral process; amp, anteromedial process; asf, articulation surface with the frontal; asp, articulation surface with the premaxilla. Scale bars = 1 mm.

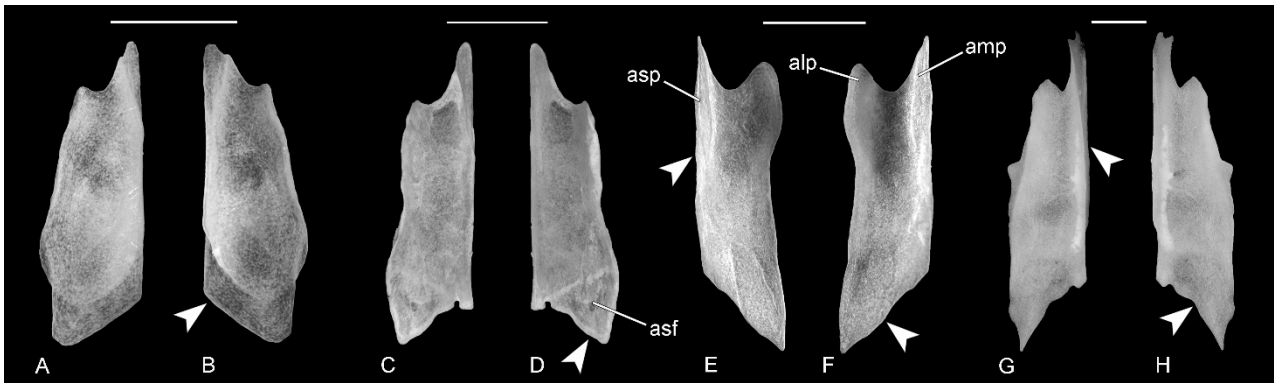


Figure 6. A-E: *E. europaea* (MDHC 389), frontal in dorsal (A), ventral (B), right lateral (C), anterior (D) and posterior (E) views. F-J: *H. turcicus* (MDHC 238), frontal in dorsal (F), ventral (G), right lateral (H), anterior (I) and posterior (J) views. K-O: *M. kotschyi* (MDHC 285), frontal in dorsal (K), ventral (L), right lateral (M), anterior (N) and posterior (O) views. P-T: *T. mauritanica* (MDHC 97), frontal in dorsal (P), ventral (Q), left lateral (R), anterior (S) and posterior (T) views. The arrows mark important diagnostic structures. Abbreviations: ap, anterior process; asmp, articulation surface with maxilla and prefrontal; asn, articulation surface with the nasal; asp, articulation surface with the postorbitofrontal; cc, crista cranii; g, groove; lp, lateral process; mp, medial process; plp, posterolateral process. Scale bars = 1 mm.

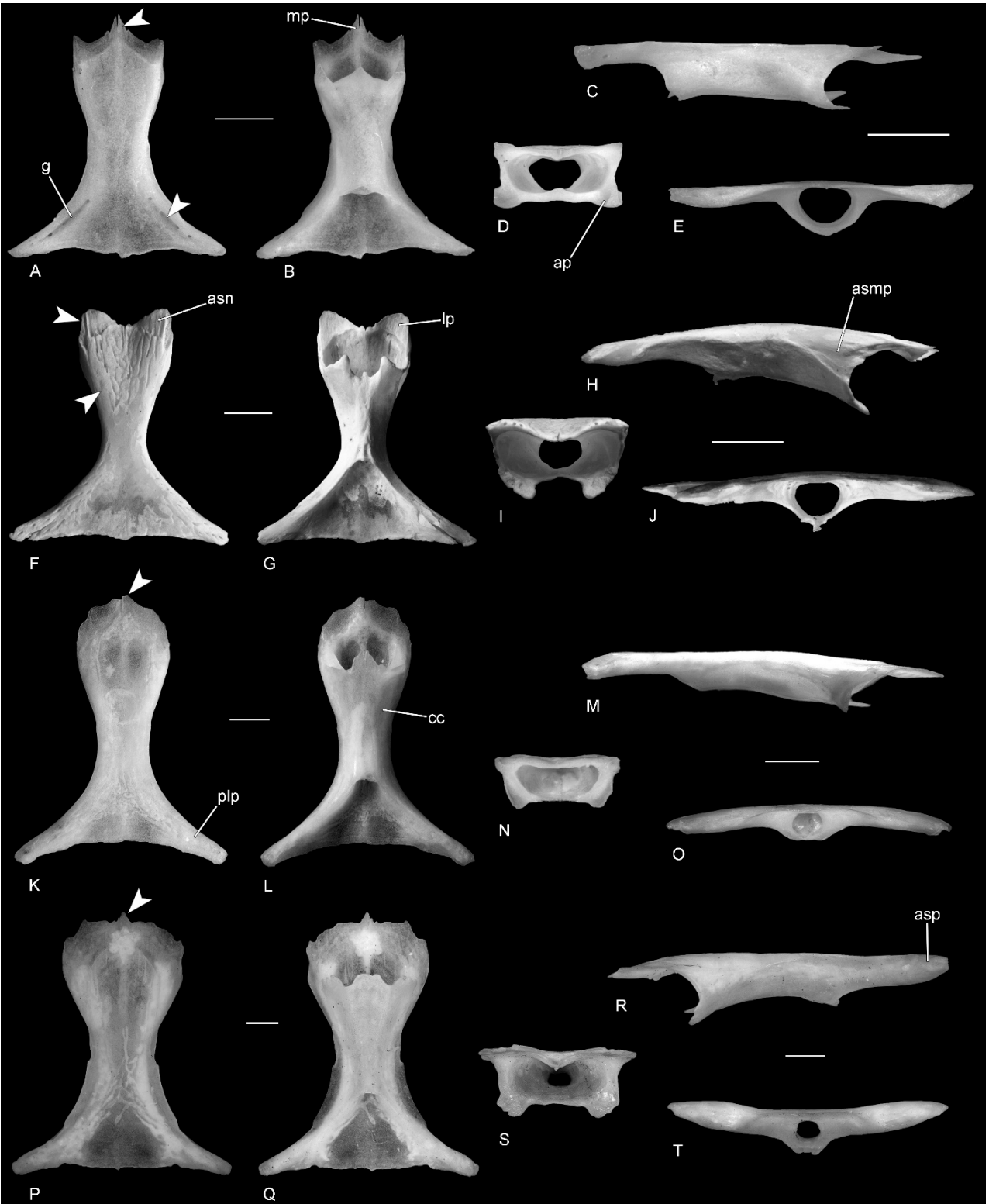


Figure 7. Partial skull of *H. turcicus* (MDHC 26) in dorsal view, showing the light ornamentation (marked by arrows) on frontal, parietals, maxillae and prefrontals. Scale bar = 1 mm.



Figure 8. A-C: *E. europaea* (MDHC 384), left parietal in dorsal (A), ventral (B) and lateral (C) views. D-F: *H. turcicus* (JDD 326–327), right parietal in ventral (D), dorsal (E) and lateral (F) views. G-I: *M. kotschyi* (MDHC 285), right parietal in ventral (G), dorsal (H) and lateral (I) views (the anteromedial corner is broken). J-L: *T. mauritanica* (MDHC 97), right parietal in ventral (J), dorsal (K) and lateral (L) views. The ornamentation is present only in *H. turcicus*, all other species have smooth surfaces. The structures that appears like grooves on the parietals of other species are inner cavities in the bones that are visible externally because of their thin aspect. The arrows mark important diagnostic structures. Abbreviations: alp, anterolateral process; ep, epipterygoid process; l, lamina; ppp, postparietal process. Scale bars = 1 mm.

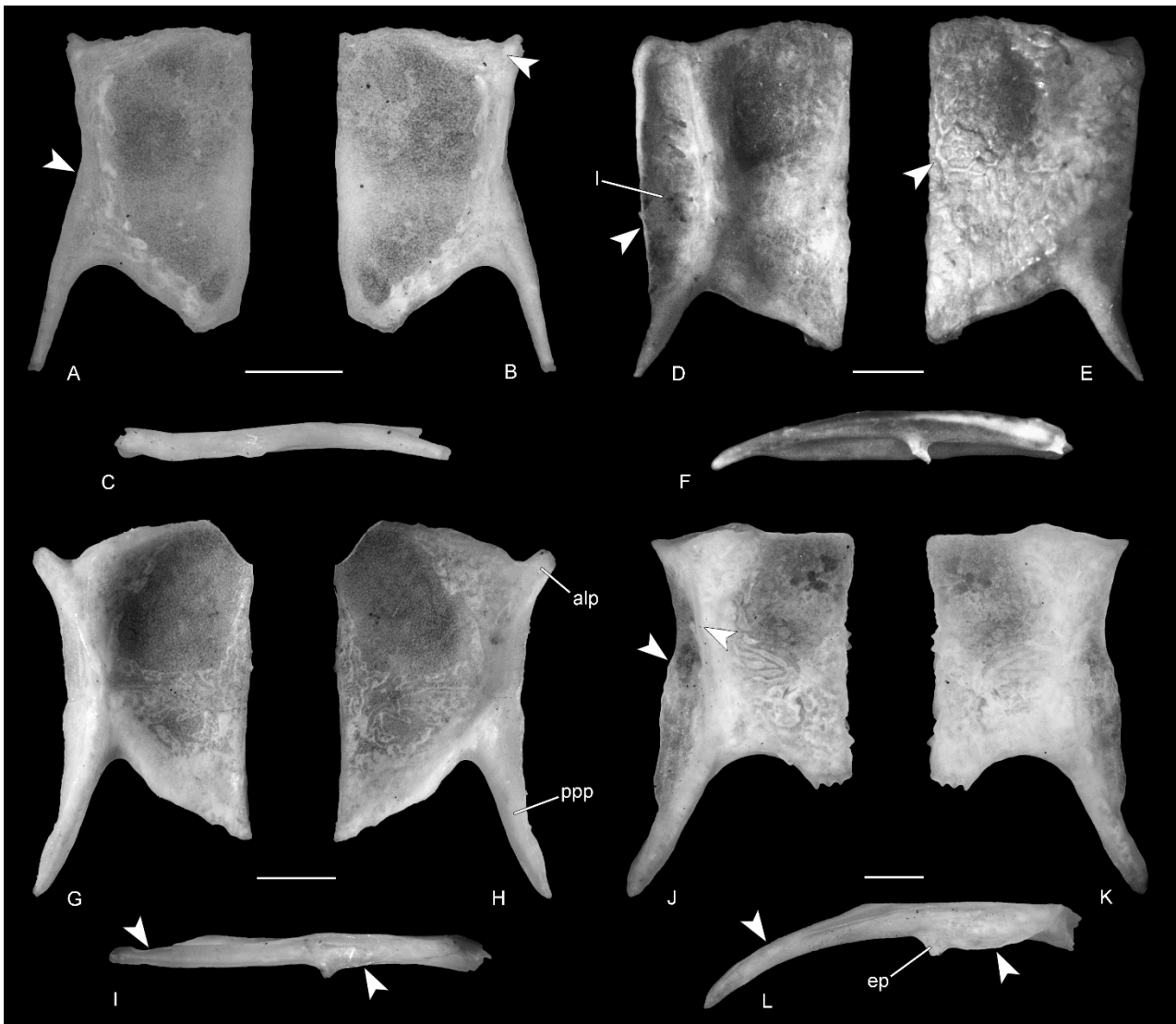


Figure 9. A-E: *E. europaea* (MDHC 388), premaxilla in anterior (A), dorsal (B), left lateral (C), ventral (D) and posterior (E) views. F-J: *H. turcicus* (JDD 326–327), premaxilla in anterior (F), dorsal (G), right lateral (H), ventral (I) and posterior (J) views. K-O: *M. kotschy* (MDHC 285), premaxilla in anterior (K), dorsal (L), right lateral (M), ventral (N) and posterior (O) views. P-T: *T. mauritanica* (MDHC 194), premaxilla in anterior (P), dorsal (Q), left lateral (R), ventral (S) and posterior (T) views. The arrows mark important diagnostic structures. Abbreviations: am, alveolar margin; anp, ascending nasal process; ap, alveolar plate; flc, foramen of the longitudinal canal; pp, palatal process; sc, septonasal crest. Scale bars = 1 mm.

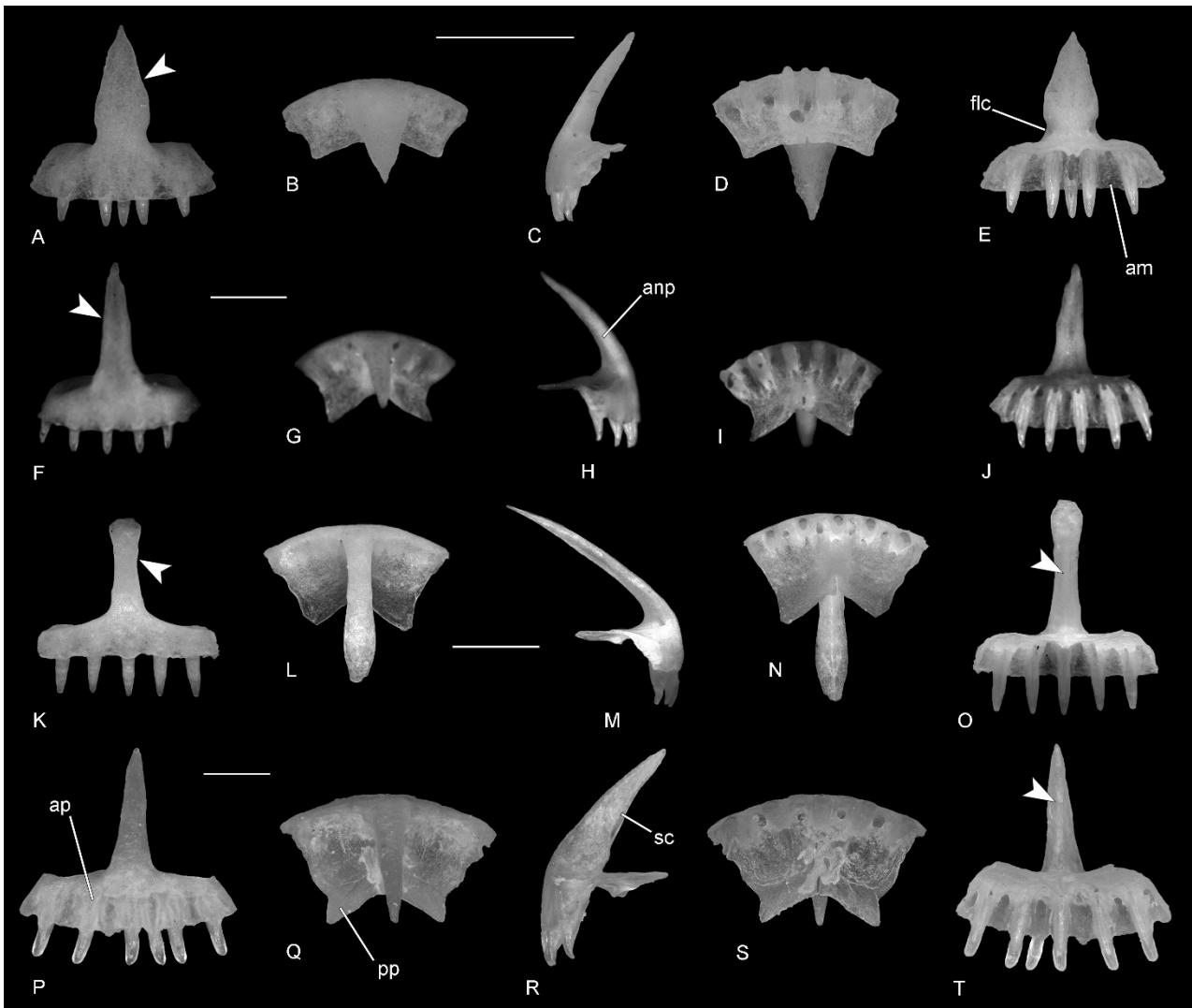


Figure 10. A-C: *E. europaea* (MDHC 389), right maxilla in lateral (A), medial (B) and dorsal (C) views. D-F: *H. turcicus* (JDD 326–327), left maxilla in lateral (D), medial (E) and dorsal (F) views. G: *M. kotschy* (MDHC 285), left maxilla in lateral view. H-I: *M. kotschy* (MDHC 201), left maxilla in medial (H) and dorsal (I) views. J-L: *T. mauritanica* (MDHC 302), right maxilla in lateral (J), medial (K) and dorsal (L) views. The arrows mark important diagnostic structures. Abbreviations: ab, alveolar border; alp, anterolateral process; amp, anteromedial process; ap, alveolar portion; app, anterior premaxillary process; fp, facial process; mr, medial ridge; pdp, postero-dorsal projection of the facial process; pp, posterior process; ps, palatal shelf; sdf, superior dental foramen; vlf, ventrolateral foramen; vnf, vomeronasal foramen. Scale bars = 1 mm.

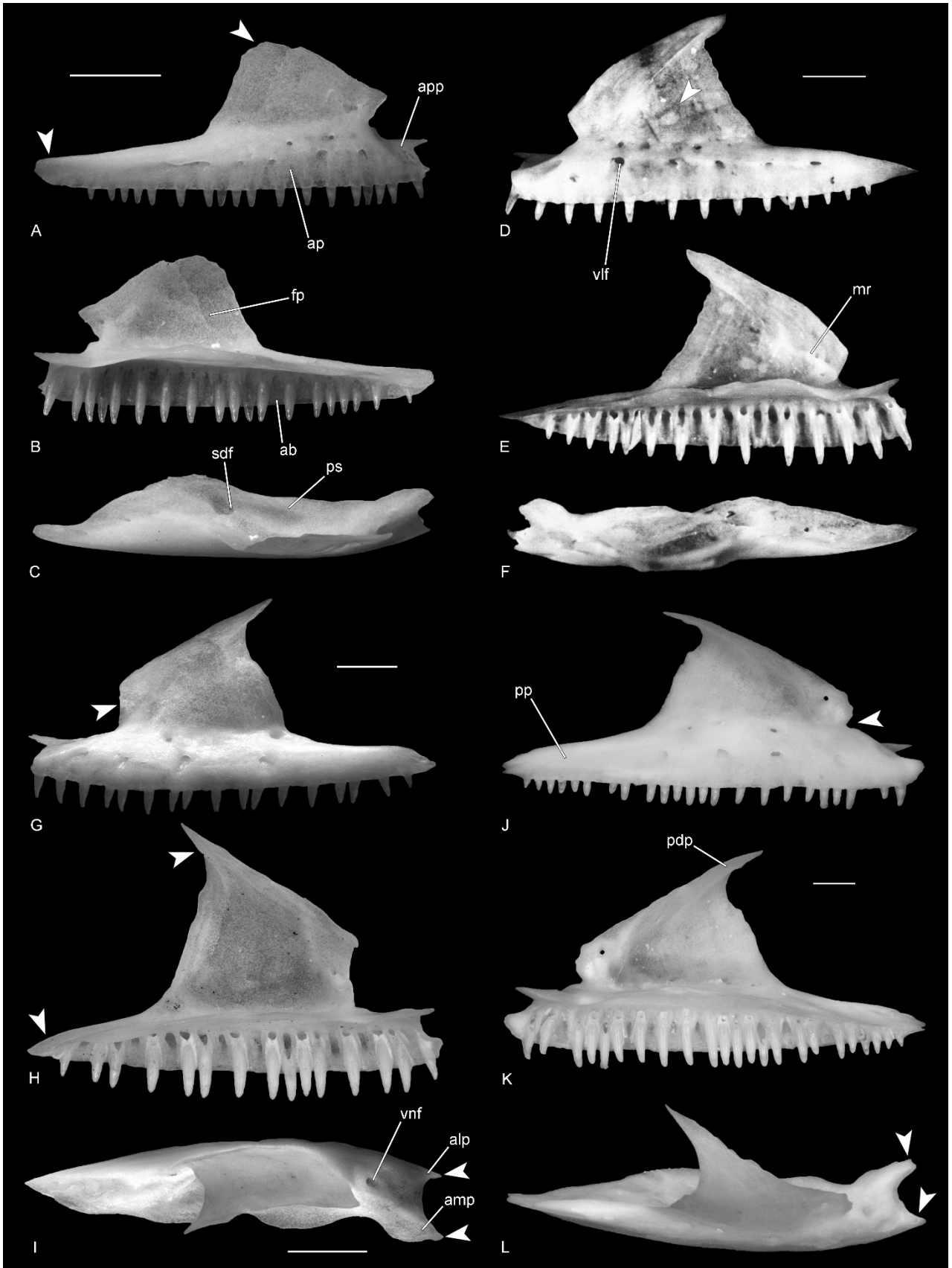


Figure 11. Left maxilla of *H. turcicus* (MDHC 238) in medial view, showing the sigmoid medial ridge (mr) on the medial surface and the groove of the lacrimal foramen (marked by an arrow).

Scale bar = 1 mm.



Figure 12. A-D: *E. europaea* (MDHC 388), left prefrontal in dorsal (A), anterior (B), lateral (C) and posterior (D) views. E-H: *H. turcicus* (MDHC 238), right prefrontal in dorsal (E), anterior (F), lateral (G) and posterior (H) views. I-L: *M. kotschyi* (MDHC 285), right prefrontal in dorsal (I), anterior (J), lateral (K) and posterior (L) views. M-P: *T. mauritanica* (MDHC 97), right prefrontal in dorsal (M), anterior (N), lateral (O) and posterior (P) views. The arrows mark important diagnostic structures. Abbreviations: adp, anterodorsal process; dp, dorsal process; nlf, notch of the lacrimal foramen; of, orbitonasal flange; ofp, orbitonasal flange projection; pvp, posteroventral process. Scale bars = 1 mm.

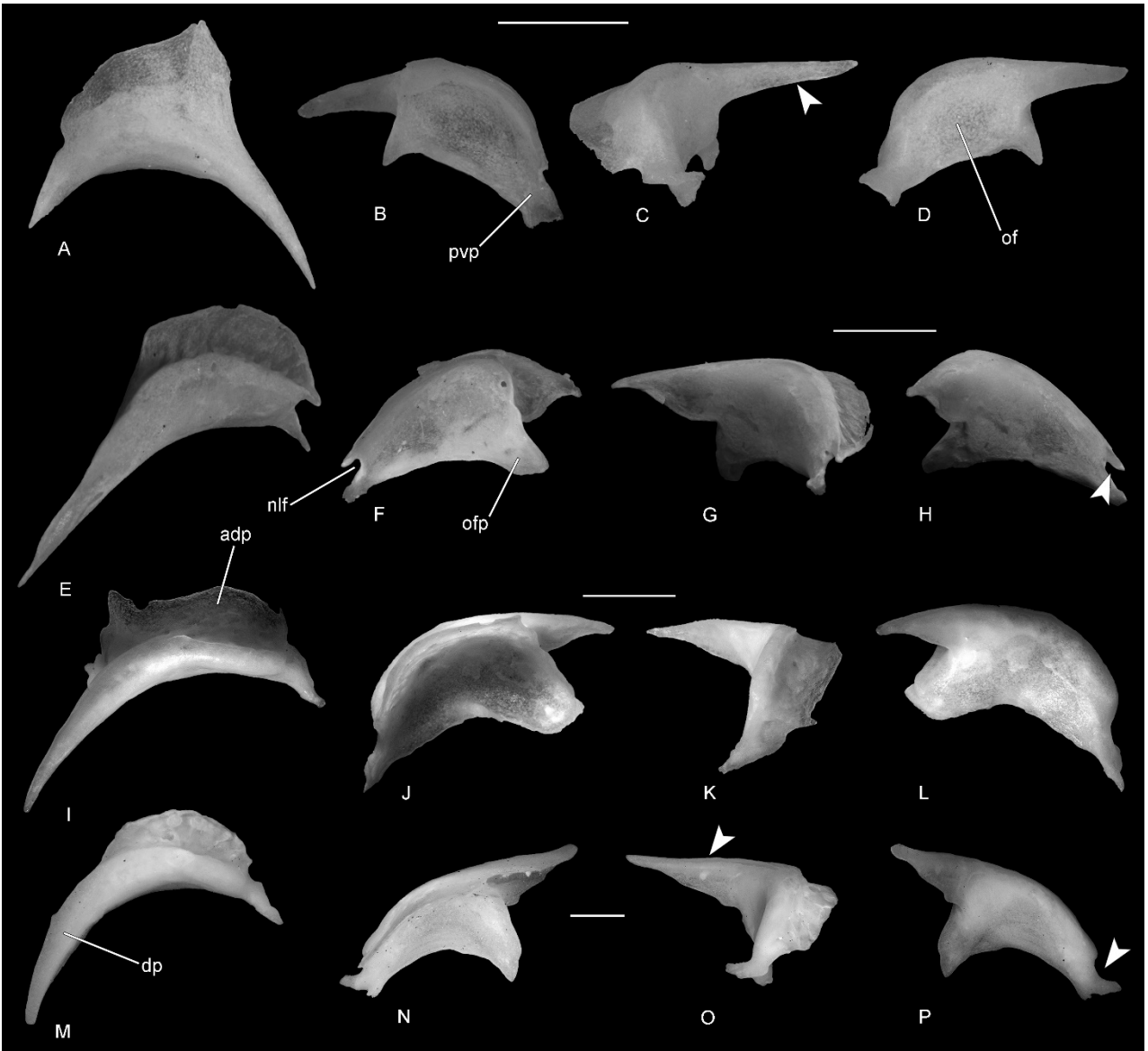


Figure 13. A-B: *E. europaea* (MDHC 388), left jugal in dorsal (A) and ventral (B) views. C-D: *H. turcicus* (MDHC 238), right jugal in dorsal (C) and ventral (D) views. E-F: *M. kotschyi* (MDHC 285), left jugal in dorsal (E) and ventral (F) views. G: *T. mauritanica* (NHMW 31945), right jugal in dorsal view. The arrows mark important diagnostic structures. Abbreviations: e, ectopterygoid; j, jugal; m, maxilla. Scale bars = 1 mm.

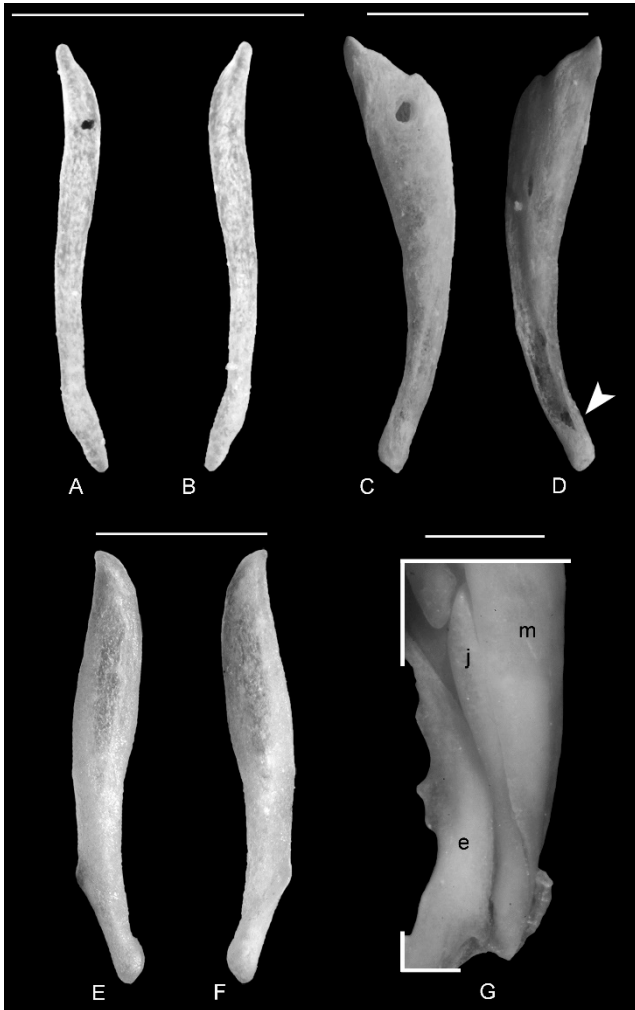


Figure 14. A-B: *E. europaea* (MDHC 388), left postorbitofrontal in dorsal (A) and ventral (B) views. C-D: *H. turcicus* (MDHC 238), left postorbitofrontal in dorsal (C) and ventral (D) views. E-F: *M. kotschy* (MDHC 285), right postorbitofrontal in dorsal (E) and ventral views (F). G-H: *T. mauritanica* (MDHC 97), left postorbitofrontal in dorsal (G) and ventral (H) views. I-J: *T. mauritanica* (MDHC 97), right squamosal in lateral (I) and medial (J) views. The arrows mark important diagnostic structures. Abbreviations: ap, anterior process; lp, lateral process; pp, posterior process. Scale bars = 1 mm.

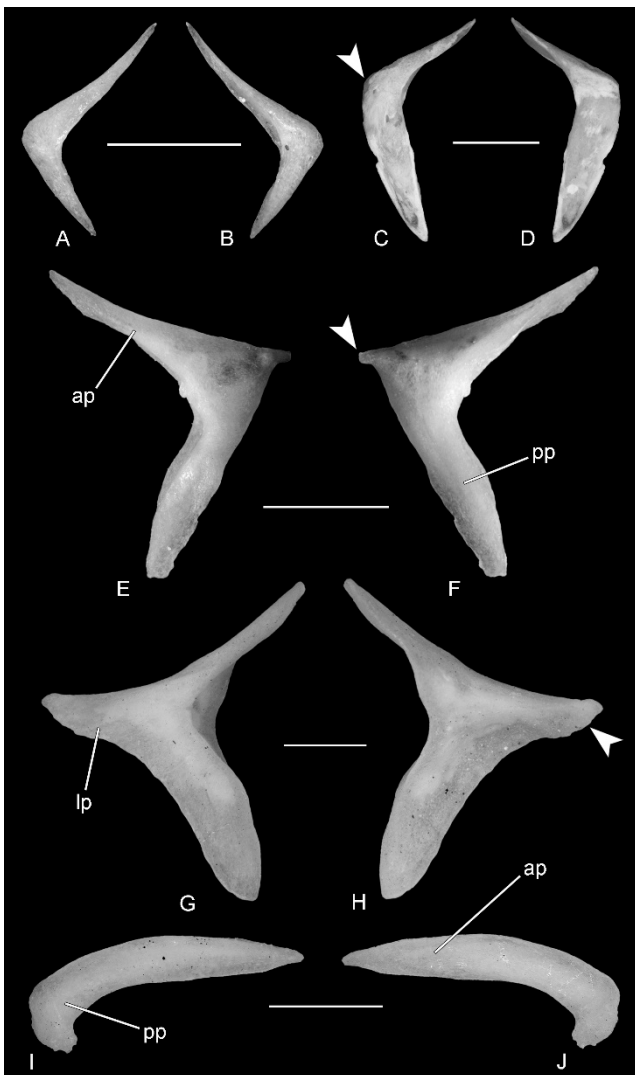


Figure 15. A-C: *E. europaea* (MDHC 388), right quadrate in posterior (A), anterior (B) and lateral (C) views. D-F: *H. turcicus* (JDD 326–327), right quadrate in posterior (D), anterior (E) and lateral (F) views. G-I: *M. kotschyi* (MDHC 285), right quadrate in posterior (G), anterior (H) and lateral (I) views. J-L: *T. mauritanica* (MDHC 97), left quadrate in posterior (J), anterior (K) and lateral (L) views. M: *T. mauritanica* (MDHC 97), epipterygoid. The arrows mark important diagnostic structures. Abbreviations: c, conch; cc, cephalic condyle; mc, mandibular condyle; p, pillar; qf, quadrate foramen; sn, squamosal notch; tc, tympanic crest. Scale bars = 1 mm.

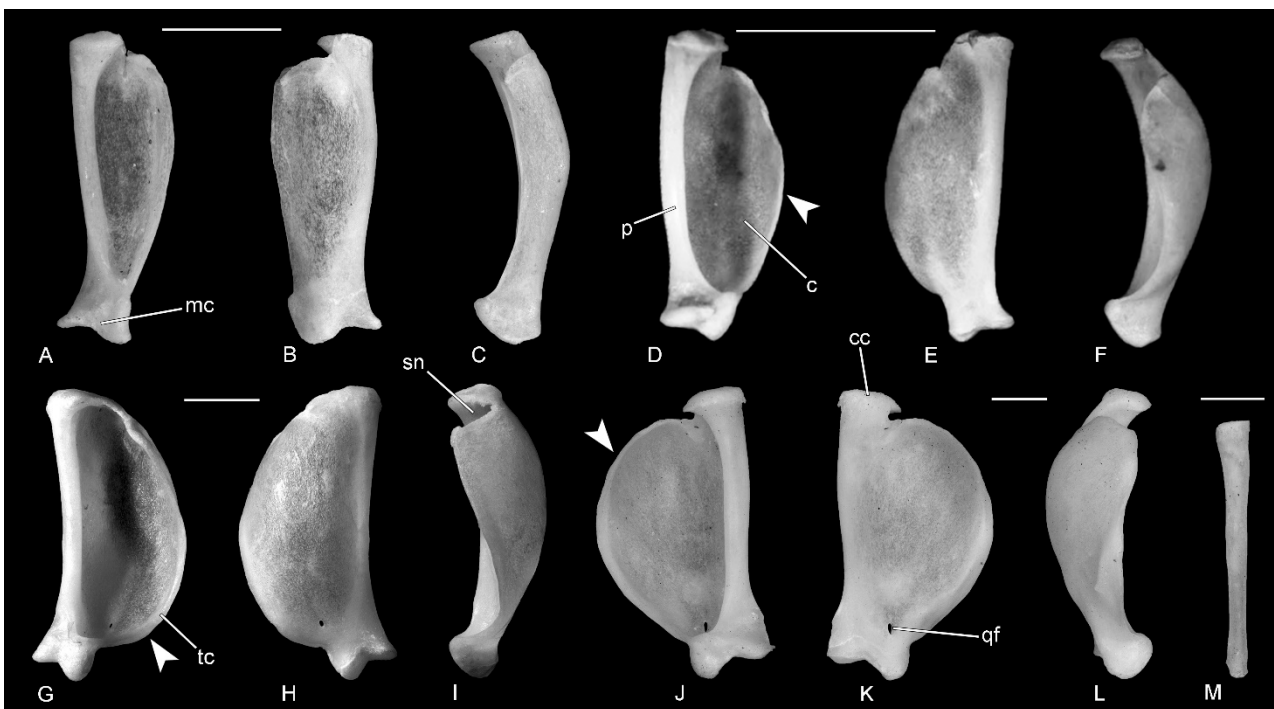


Figure 16. A-B: *E. europaea* (MDHC 384), right vomer in ventral (A) and dorsal (B) views. C-D: *H. turcicus* (JDD 326–327), right vomer in ventral (C) and dorsal (D) views. E-F: *M. kotschy* (MDHC 285), left vomer in ventral (E) and dorsal (F) views. G-H: *T. mauritanica* (MDHC 302), right vomer in ventral (G) and dorsal (H) views. I-L: *E. europaea* (MDHC 384), left septomaxilla in dorsal (I), ventral (J), lateral (K) and medial (L) views. M-P: *H. turcicus* (JDD 326–327), right septomaxilla in dorsal (M), ventral (N), lateral (O) and medial (P) views. Q-S: *M. kotschy* (MDHC 285), right septomaxilla in dorsal (Q), ventral (R) and lateral (S) views. T: *M. kotschy* (MDHC 285), left septomaxilla in medial view. U-X: *T. mauritanica* (MDHC 302), left septomaxilla in dorsal (U), ventral (V), lateral (W) and medial (X) views. The arrows mark important diagnostic structures. Abbreviations: ar, arched ridge; g, groove; lp, lateral process; lr, lateral ridge; mp, medial process; mr, medial ridge; nr, nasal region; nvf, notch of the vomeronasal fenestra; tp, triangular process; vr, vomeronasal region. Scale bars = 1 mm.

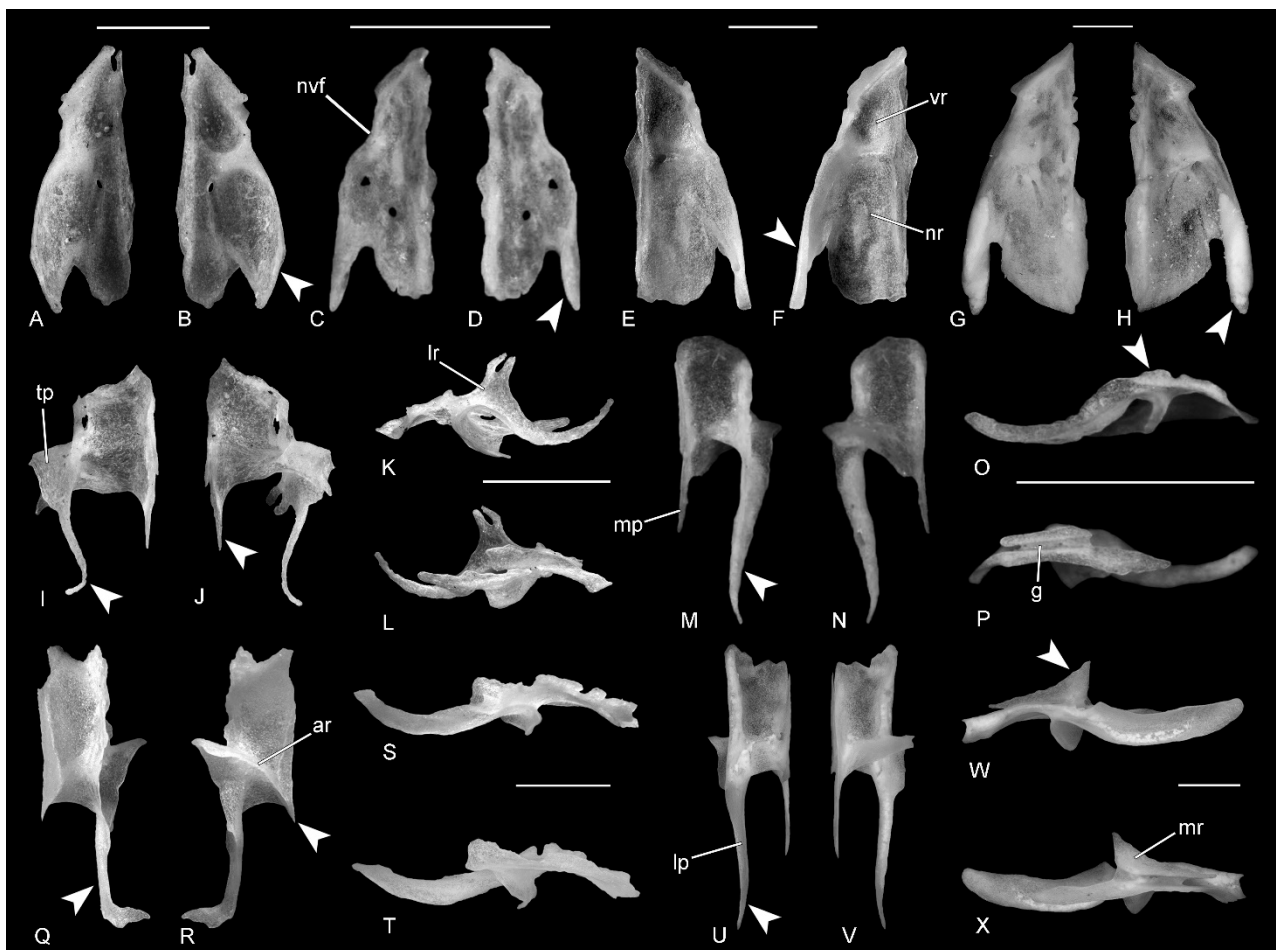


Figure 17. A-B: *E. europaea* (MDHC 384), right palatine in dorsal (A) and ventral (B) views. C-D: *H. turcicus* (JDD 326–327), left palatine in dorsal (C) and ventral (D) views. E-F: *M. kotschyi* (MDHC 285), left palatine in dorsal (E) and ventral (F) views. G-H: *T. mauritanica* (MDHC 97), right palatine in dorsal (G) and ventral (H) views. I-J: *E. europaea* (MDHC 384), left pterygoid in dorsal (I) and ventral (J) views. K-L: *H. turcicus* (JDD 326–327), left pterygoid in dorsal (K) and ventral (L) views. M-N: *M. kotschyi* (MDHC 285), right pterygoid in dorsal (M) and ventral (N) views. O-P: *T. mauritanica* (MDHC 97), right pterygoid in dorsal (O) and ventral (P) views. Q-R: *E. europaea* (MDHC 388), right ectopterygoid in ventral (Q) and dorsal (R) views. S-T: *H. turcicus* (JDD 326–327), left ectopterygoid in dorsal (S) and ventral (T) views. U-V: *M. kotschyi* (MDHC 285), right ectopterygoid in ventral (U) and dorsal (V) views. W-X: *T. mauritanica* (MDHC 97), right ectopterygoid in ventral (W) and dorsal (X) views. The arrows mark important diagnostic structures. Abbreviations: alp, anterolateral process; bf, basipterygoid fossa; cd, choanal duct; dr, dorsal ridge; fc, fossa columellae; mp, maxillary process; pap, palatine process; pf, pterygoid flange; pmp, posteromedial process; pr, pterygoid recess; ptp, pterygoid process; qp, quadrate process; vp, vomerine process; vr, ventral ridge. Scale bars = 1 mm.

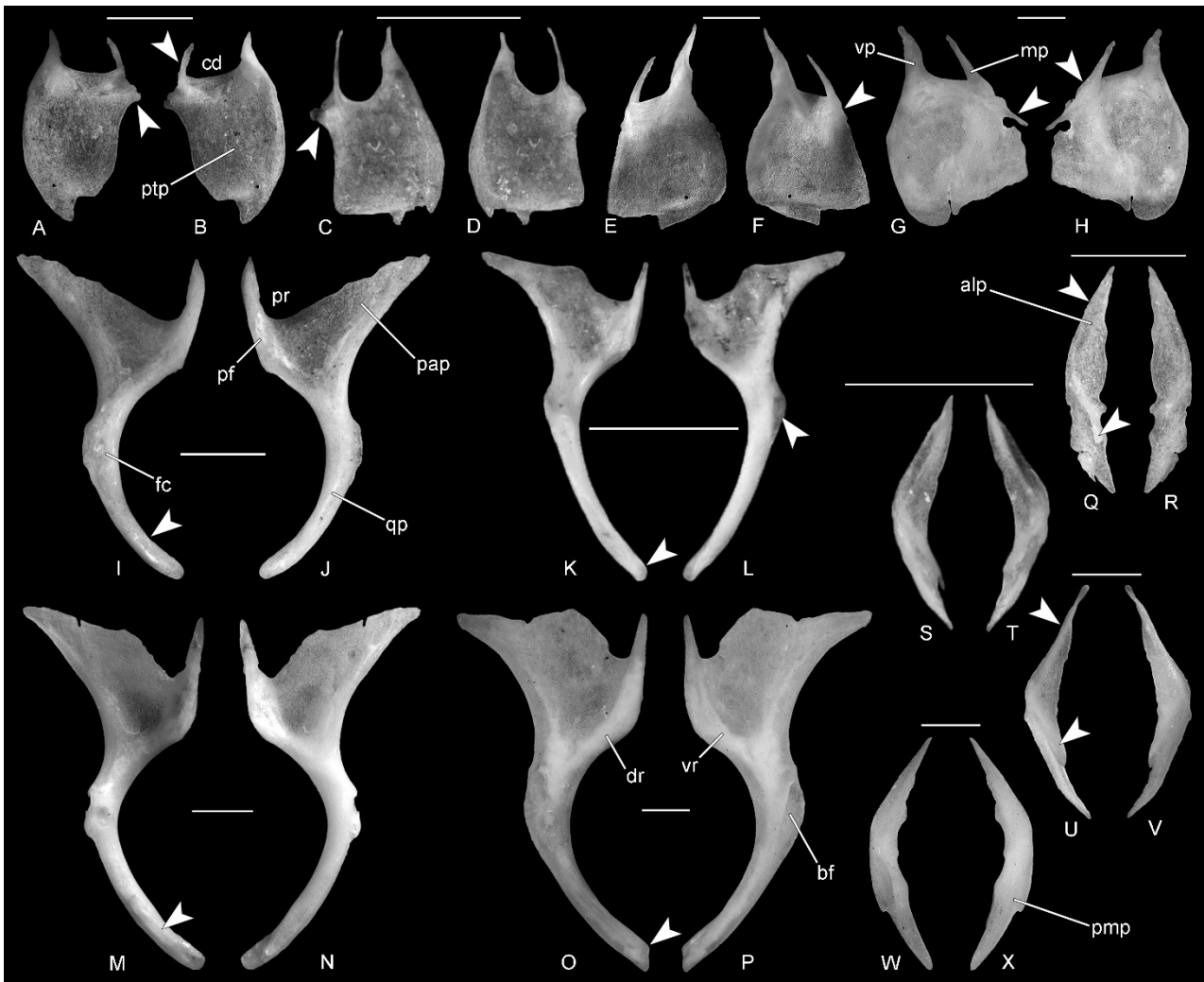


Figure 18. A-E: *E. europaea* (MDHC 384), otooccipital region in anterior (A), left lateral (B), posterior (C), dorsal (D) and ventral (E) views. F-J: *H. turcicus* (MDHC 26), otooccipital region in anterior (F), left lateral (G), posterior (H), dorsal (I) and ventral (J) views. The arrows mark important diagnostic structures. Abbreviations: asc, anterior semicircular canal; b, basioccipital; bp, basipterygoid process; cc, cochlear cavity; fma, foramen magnum; fo, fenestra ovalis; hsc, horizontal semicircular canal; o, otooccipital; oc, occipital condyle; p, prootic; pap, paroccipital process; pf, perilymphatic foramen; psc, posterior semicircular canal; sp, sphenoid; su, supraoccipital; svp, supravenuous process; tc, trabecula cranii. Scale bars = 1 mm.

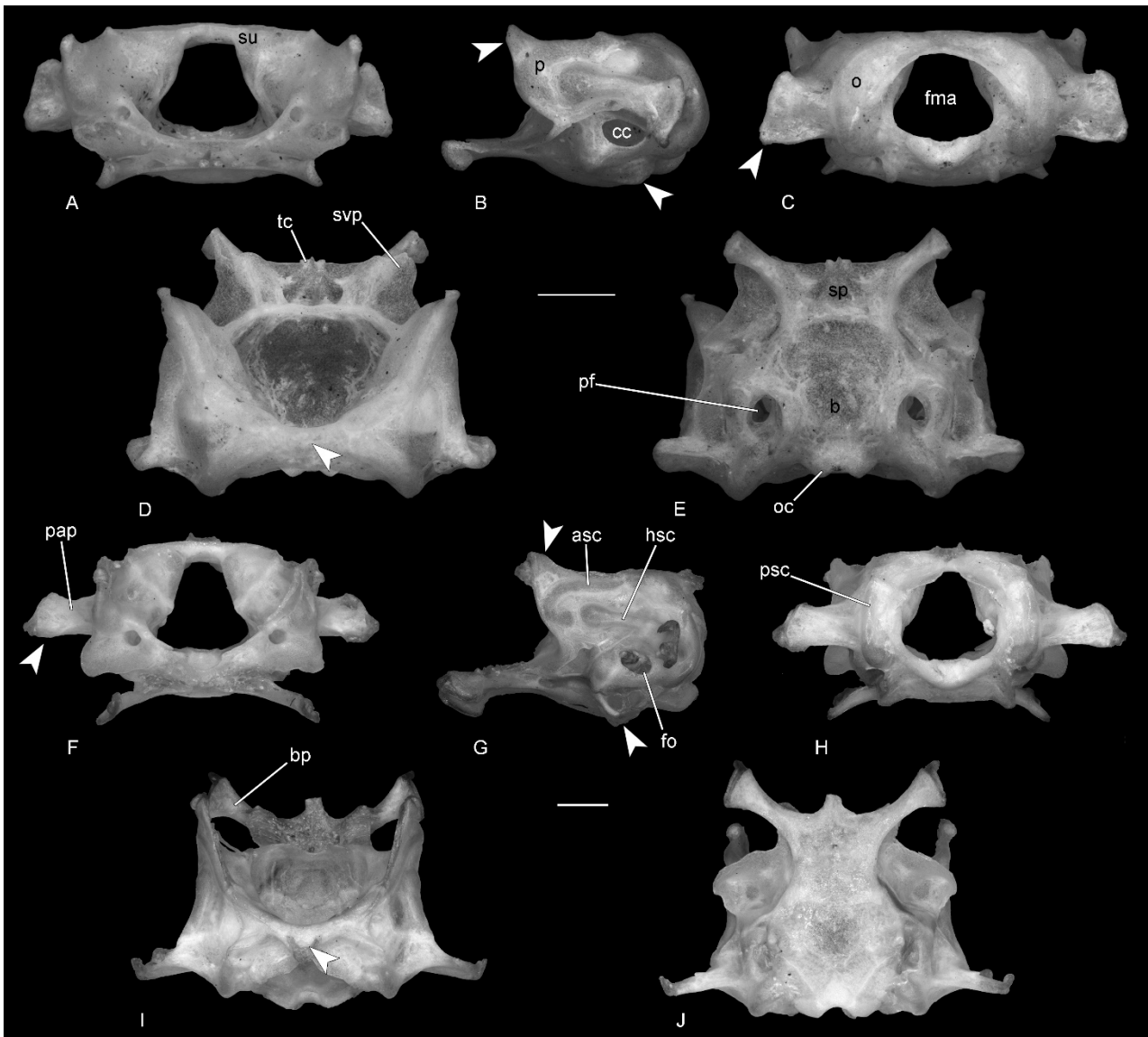


Figure 19. A-E: *M. kotschy* (MDHC 285), otooccipital region in anterior (A), left lateral (B), posterior (C), dorsal (D) and ventral (E) views. F-J: *T. mauritanica* (MDHC 97), otooccipital region in anterior (F), left lateral (G), posterior (H), dorsal (I) and ventral (J) views. The arrows mark important diagnostic structures. Abbreviations: aovc, anterior opening of the vidian canal; ap, alar process; ca, crista alaris; ci, crista interfenestralis; cp, crista prootica; ctr, crista trabecularis; ctu, crista tuberalis; ff, facial foramen; glhv, groove of the lateral head vein; hf, hypophysial fossa; ip, incisura prootica; l, lamina; lrst, lateral opening of the recessus scalae tympani; povc, posterior opening of the vidian canal; pp, posterior process of the prootic; rst, recessus scalae tympani; rvj, recessus vena jugularis; st, sphenoccipital tubercle; vf, vagus foramen. Scale bars = 1 mm.

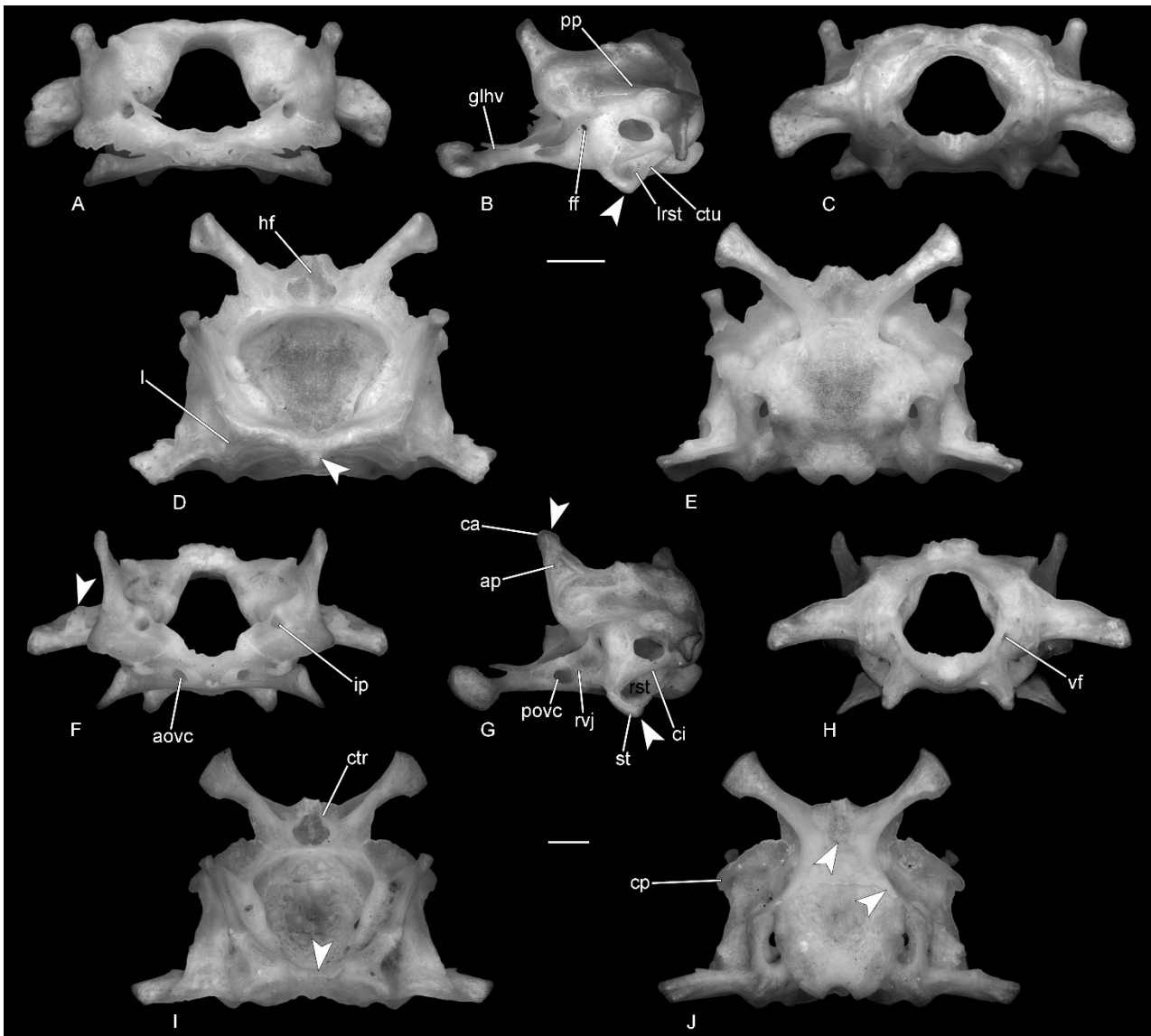


Figure 20. A-B: *T. mauritanica* (MDHC 302), basioccipital in dorsal (A) and ventral (B) views. C-D: *T. mauritanica* (MDHC 302), sphenoid in posterior (C) and dorsal (D) views. E: *T. mauritanica* (MDHC 302), supraoccipital in ventrolateral view. F-G: *T. mauritanica* (MDHC 302), left prootic in medial (F) and posterior (G) views. H-I: *T. mauritanica* (MDHC 302), right otooccipital in anterior (H) and medial (I) views. J: *T. mauritanica* (MDHC 97), stapes. Abbreviations: af, abducens foramen; aaf, anterior acoustic foramen; aip, anterior inferior process; amr, ampullary recess; ap, alar process; asc, anterior semicircular canal; cac, cavum capsularis; cc, cochlear cavity; ccr, cochlear crest; cd, cranial depression; cru, common crus; cs, crista sellaris; cv, crista ventrolateralis; ef, endolymphatic foramen; ff, facial foramen; gpd, groove for the perilymphatic

duct; hsc, horizontal semicircular canal; icf, internal carotid foramen; lw, lateral wing; mfp, medial footplate; paf, posterior acoustic foramen; ppp, posterior projection of the posterior process of the prootic; psc, posterior semicircular canal; s, shaft; sf, stapedial foramen; st, sella turcica; ur, utricular recess. Scale bars = 1 mm.

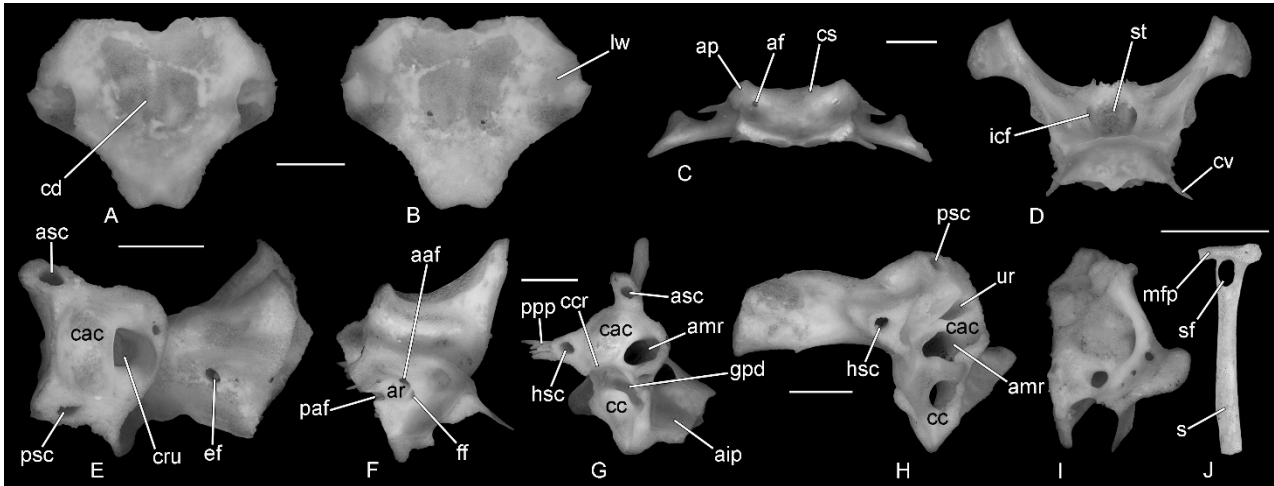


Figure 21. A-C: *E. europaea* (MDHC 384), right dentary in lateral (A), medial (B) and dorsal (C) views. D-E: *H. turcicus* (JDD 326–327), left dentary in lateral (D) and medial (E) views. F: *H. turcicus* (JDD 326–327), right dentary in dorsal view. G-I: *M. kotschy* (MDHC 285), right dentary in lateral (G), medial (H) and dorsal (I) views. J-L: *T. mauritanica* (MDHC 302), left dentary in lateral (J), medial (K) and dorsal (L) views. The arrows mark important diagnostic structures. Abbreviations: as, alveolar shelf; ip, inferior process; mef, mental foramen; mkf, Meckelian fossa; ms, mandibular symphysis; sp, superior process; sr, subdental ridge. Scale bars = 1 mm.

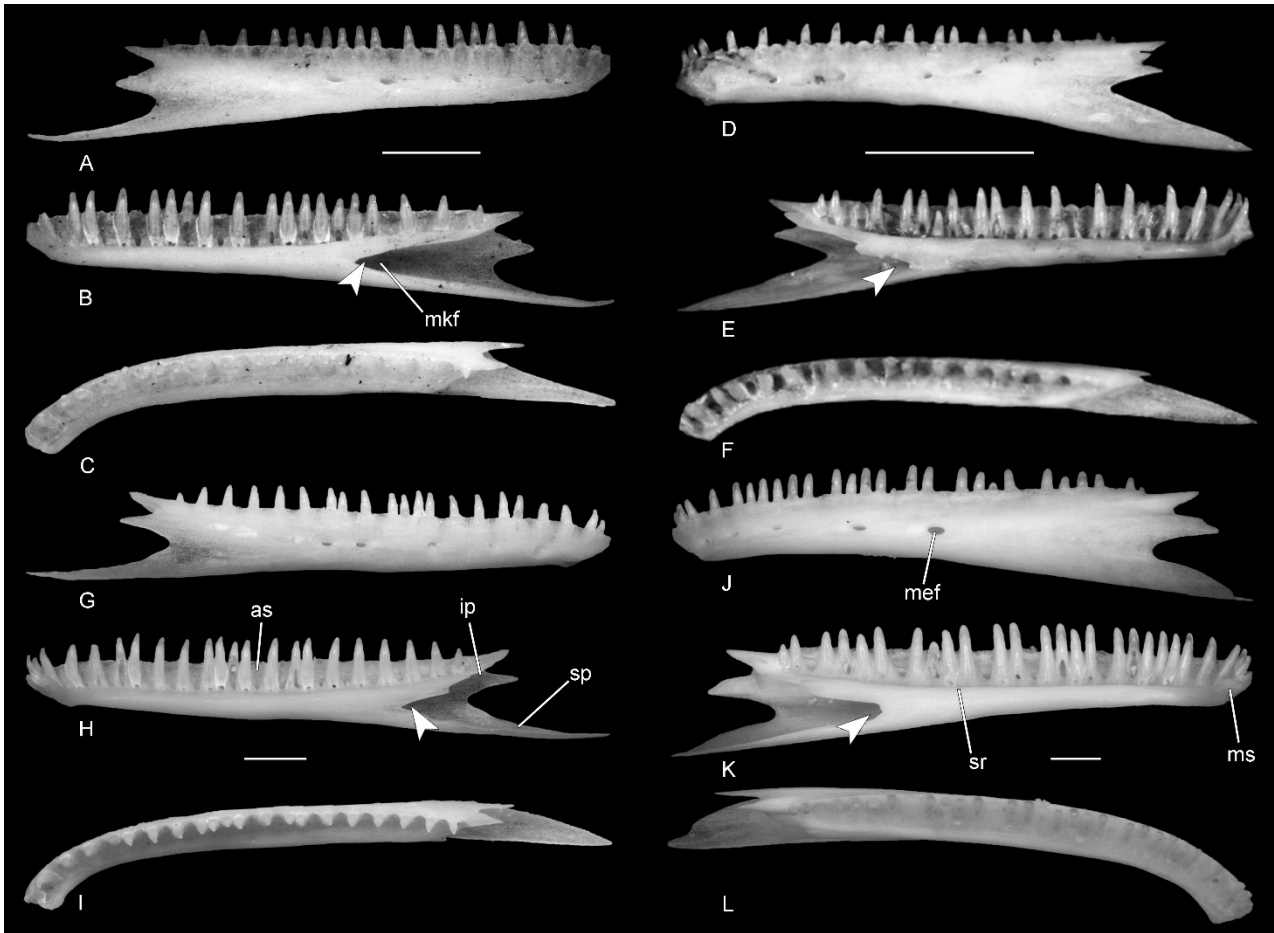


Figure 22. A-B: *E. europaea* (MDHC 384), left splenial in lateral (A) and medial (B) views. C-D: *H. turcicus* (MDHC 238), left splenial in lateral (C) and medial (D) views. E-F: *M. kotschy* (MDHC 285), right splenial in lateral (E) and medial (F) views. G-H: *T. mauritanica* (MDHC 302), right splenial in lateral (G) and medial (H) views. I-L: *E. europaea* (MDHC 388), left coronoid in dorsal (I), ventral (J), lateral (K) and medial (L) views. M-P: *H. turcicus* (MDHC 238), left coronoid in dorsal (M), ventral (N), lateral (O) and medial (P) views. Q-T: *M. kotschy* (MDHC 285), right coronoid in dorsal (Q), ventral (R), lateral (S) and medial (T) views. U-X: *T. mauritanica* (MDHC 302), right coronoid in dorsal (U), ventral (V), lateral (W) and medial (X) views. The arrows mark important diagnostic structures. Abbreviations: aif, anterior inferior foramen; amf, anterior mylohyoid foramen; amp, anteromedial process; cp, coronoid process; lp, labial process; pmp, posteromedial process. Scale bars = 1 mm.

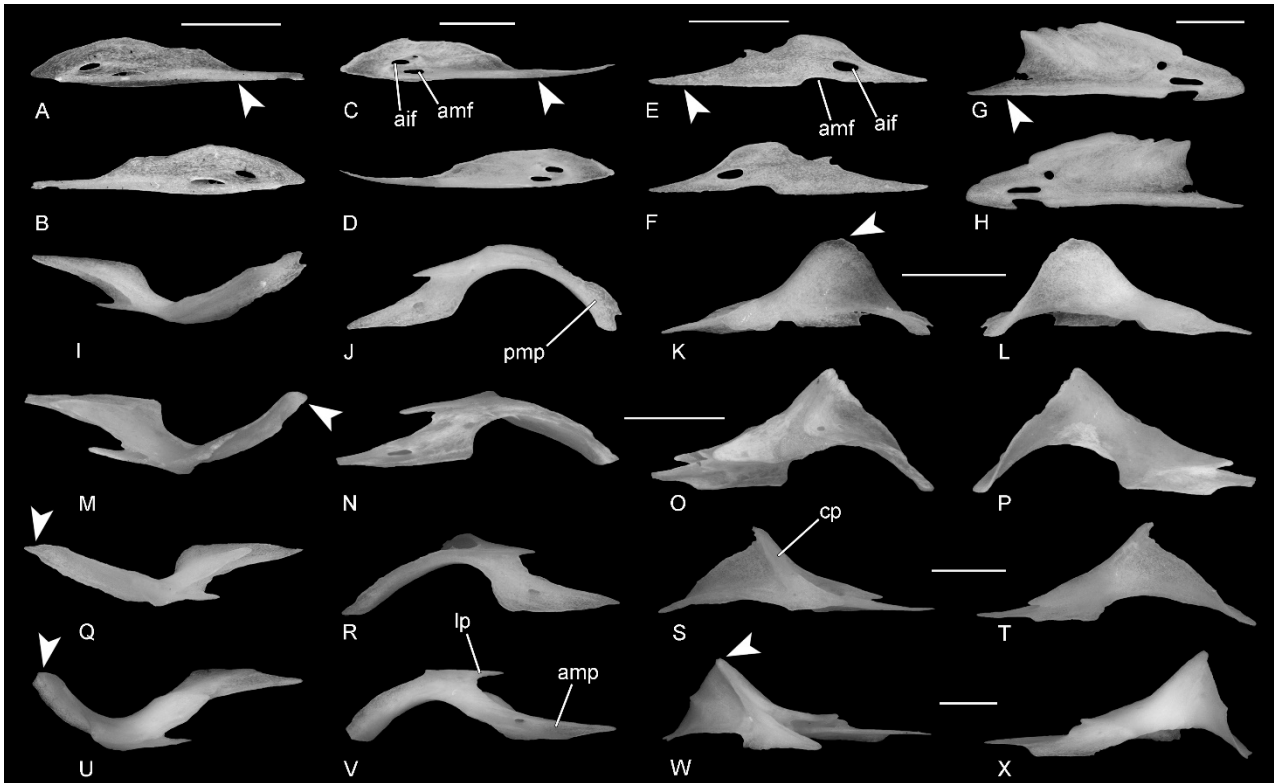


Figure 23. A-C: *E. europaea* (MDHC 388), left compound bone in medial (A), lateral (B) and dorsal (C) views. D-F: *H. turcicus* (JDD 326–327), left compound bone in medial (D), lateral (E) and dorsal (F) views. G-I: *M. kotschyi* (MDHC 285), left compound bone in medial (G), lateral (H) and dorsal (I) views. J-L: *T. mauritanica* (MDHC 302), right compound bone in medial (J), lateral (K) and dorsal (L) views. The arrows mark important diagnostic structures. Abbreviations: ac, articular condyle; af, adductor fossa; asf, anterior surangular foramen; fct, foramen for the chorda tympani; lc, lateral crest; psf, posterior surangular foramen; rp, retroarticular process. Scale bars = 1 mm.

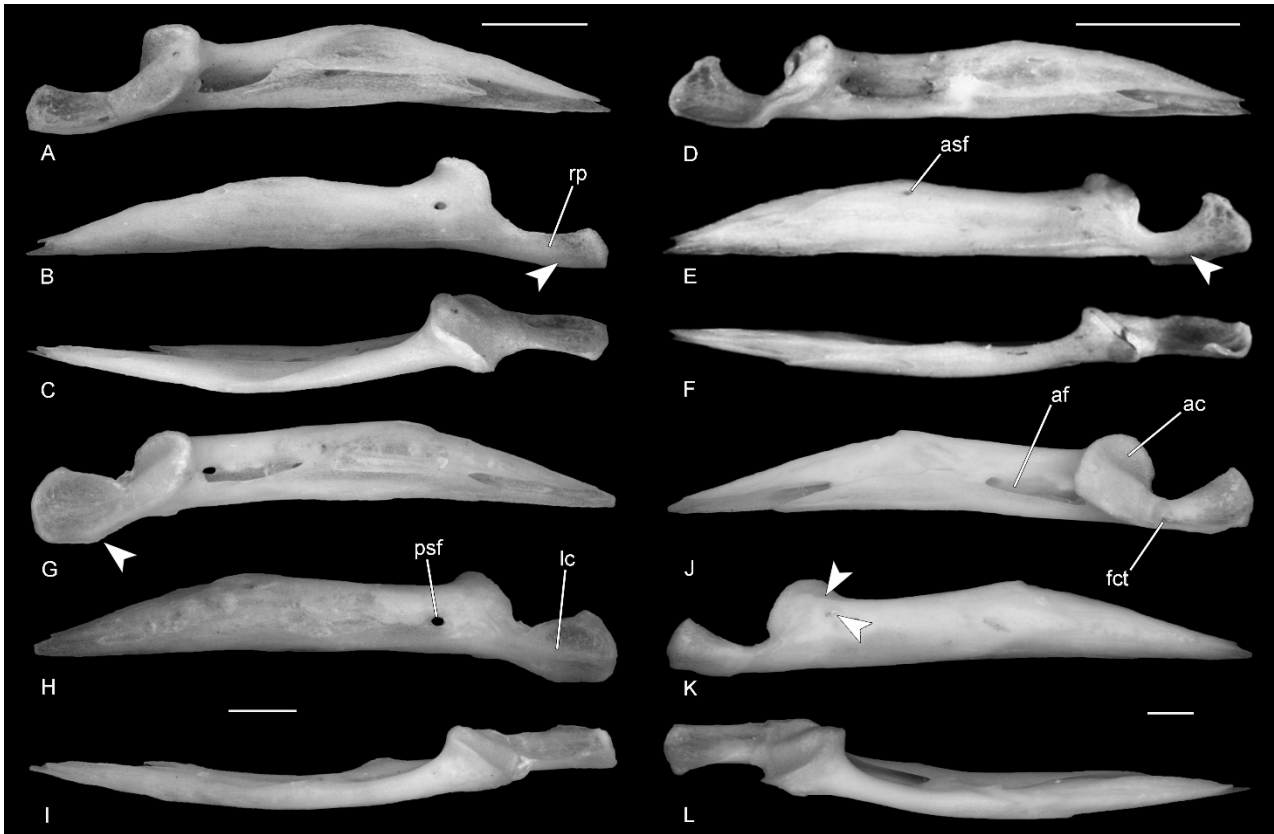


Figure 24. Dentary teeth in lingual view. A: *E. europaea* (MDHC 384). B: *H. turcicus* (MDHC 26). C: *M. kotschyi* (MDHC 201). D: *T. mauritanica* (MDHC 119). E: *C. chalcides* (MDHC 94). F: *C. cordylus* (NHMW 707). Abbreviations: ai, antrum intercristatum; ci, carina intercuspidalis; cl, culmen lateris; cla, cuspis labialis; cli, cuspis lingualis; le, lateral edge; me, medial edge. The black arrow marks a stria on the lingual side of the tooth in *C. chalcides*. Scale bar for *C. cordylus* is 1 mm.

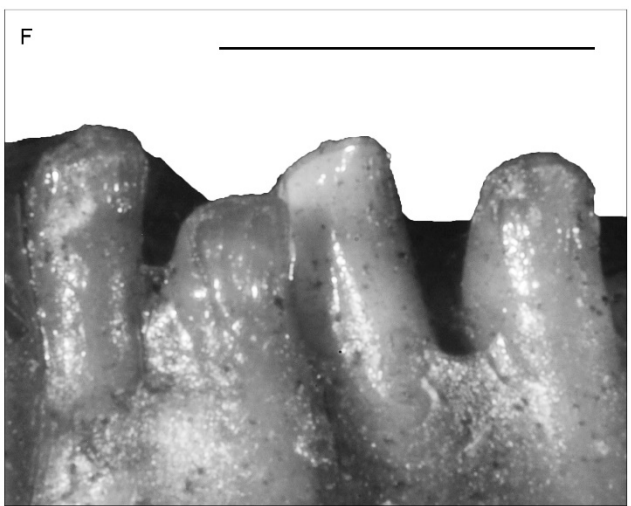
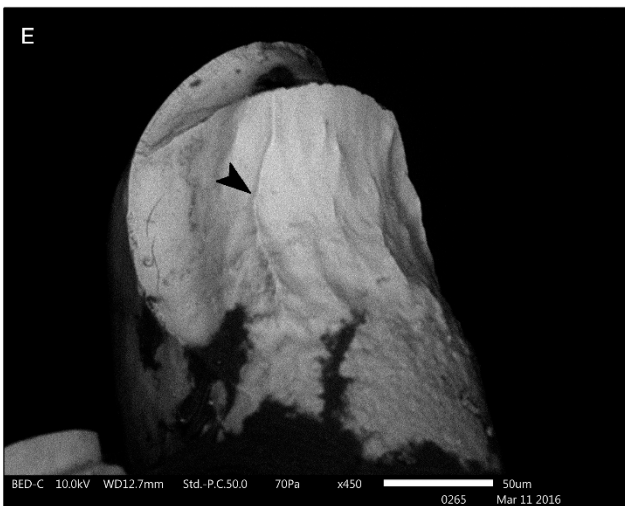
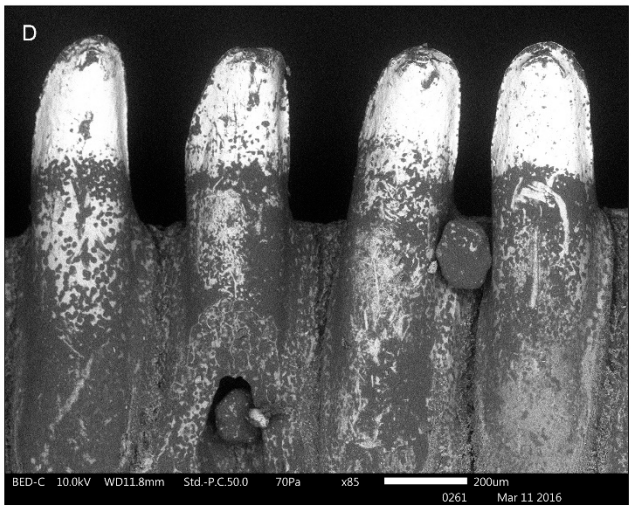
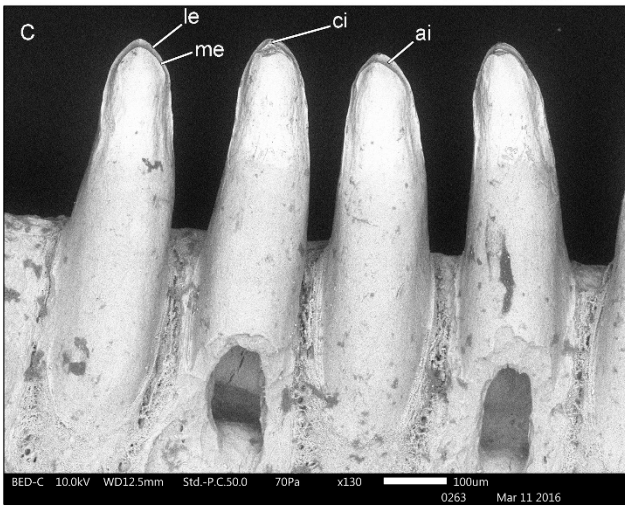
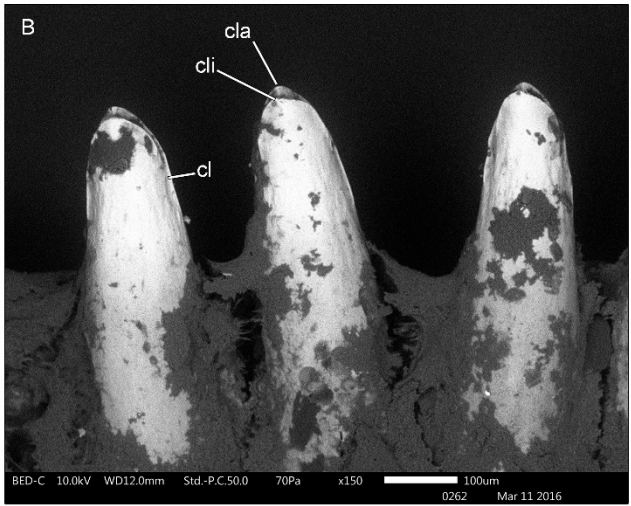
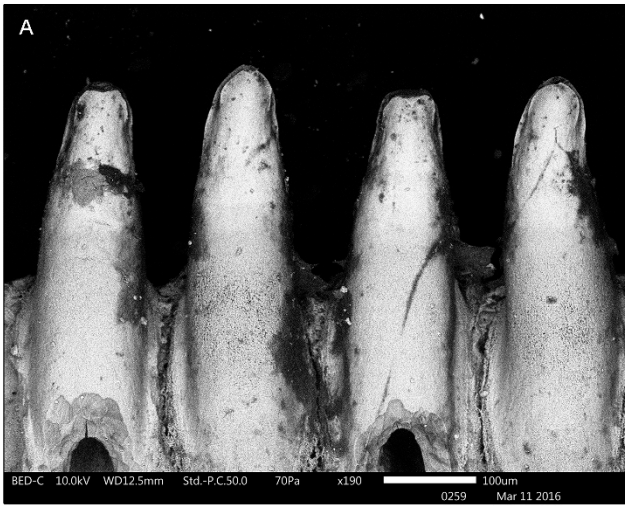


TABLE CAPTIONS

Table 1. Measurements of the examined specimens. All values are in mm.

| | <i>E. europaea</i> | <i>H. turcicus</i> | <i>M. kotschyi</i> | <i>T. mauritanica</i> |
|--|--------------------|--------------------|--------------------|-----------------------|
| Maximum length of the frontal | 4 - 4.5 | 5 - 6 | 5 - 6 | 7 - 9.1 |
| Maximum length of the parietal | 3 - 3.2 | 3.5 - 4.5 | 3.5 - 4 | 3.9 - 5.1 |
| Maximum width of the parietal | 2 | 2.5 - 2.9 | 2 - 2.9 | 2.9 - 4 |
| Maximum length of the alveolar plate of the premaxilla | 1.4 - 1.5 | 1.9 - 2 | 1.9 - 2 | 2.7 - 3.5 |
| Maximum length of the alveolar border of the maxilla | 4.3 - 5 | 5 - 6.6 | 5.2 - 6.8 | 7.9 - 10.5 |
| Maximum length of the quadrate | 2.5 - 3 | 2.9 - 4 | 3 - 3.9 | 4.6 - 6.3 |
| Maximum length of the pterygoid | 4 - 4.3 | 5 - 6 | 5 - 6.5 | 7.2 - 10 |
| Maximum length of the alveolar shelf of the dentary | 4.2 - 4.8 | 6 - 7 | 5.3 - 7 | 8.5 - 10.6 |

Table 2. Number of tooth positions in the studied specimens of European gekkotans. In case of paired element, the first number is referred to the left bone, whereas the second one to the right bone. / indicates that it was not possible to establish the exact number of positions because of the bad preservational condition of the bone.

| | | Premaxilla | Maxilla | Dentary |
|-----------------------|------------|-------------------|----------------|----------------|
| <i>E. europaea</i> | MDHC 384 | 8 | 27 - 26 | 29 - 28 |
| | MDHC 388 | 9 | 27 - 29 | 29 - 31 |
| | MDHC 389 | / | 29 - 28 | 30 - 32 |
| <i>H. turcicus</i> | MDHC 26 | 11 | 29 - 29 | 31 - 29 |
| | MDHC 238 | 10 | 25 - 25 | 29 - 28 |
| <i>M. kotschyi</i> | MDHC 201 | 9 | 23 - 22 | 27 - 27 |
| | MDHC 285 | 11 | 29 - 30 | 37 - 37 |
| | MDHC 418 | 11 | 27 - 26 | 33 - 31 |
| | MDHC 419 | 11 | 25 - 25 | 29 - 30 |
| <i>T. mauritanica</i> | MDHC 97 | 11 | 27 - 29 | 29 - 30 |
| | MDHC 98 | 11 | 27 - / | / - / |
| | MDHC 119 | 9 | 28 - 29 | 31 - 30 |
| | MDHC 194 | 11 | 30 - 30 | 33 - 33 |
| | MDHC 302 | 10 | 32 - 30 | 33 - 33 |
| | NHMW 2484 | / | 31 - 31 | 28 - / |
| | NHMW 31945 | 11 | 30 - 30 | 32 - 31 |